Math. Proc. Camb. Phil. Soc. (2026), **181**, 1303–1338
doi:10.1017/S0305004126102163
First published online 17 July 2026

Complex hyperbolic geometry of Chain links

BY JIMING MA
School of Mathematical Sciences, Fudan University, Shanghai 200433, *China.*
e-mail: majiming@fudan.edu.cn

BAOHUA XIE
School of Mathematics, Hunan University, Changsha 410082, *China.*
e-mail: xiexbh@hnu.edu.cn

AND MENGMENG XU
School of Mathematical Sciences, Huaqiao University, Quanzhou 362021, *China.*
e-mail: mengmengxu@hqu.edu.cn

(*Received* 27 *November* 2024 *UTC; revised* 17 *November* 2025 *UTC; accepted* 20 *April* 2026 *UTC*)

Abstract

We study the geometry of the complex hyperbolic triangle group $\Delta_{4,\infty,\infty;\infty}$ acting on the complex hyperbolic plane $\mathbf{H}^2_{\mathbb{C}}$ and show that the 3-manifold at infinity of $\Delta_{4,\infty,\infty;\infty}$ is the complement of the chain link 8^4_1 in the 3-sphere. In particular, the four-cusped hyperbolic 3-manifold $S^3 - 8^4_1$ admits a spherical CR-uniformisation. Since the ideal boundary of the Ford domain is an infinite-genus handlebody, we introduce a new technique to construct embedded topological disks that cap off the genus, ensuring their boundaries are compatible with the side-pairings. This surgical approach facilitates the determination of the fundamental group of the manifold at infinity and simplifies the computation compared to [**14**].

Based on this result and previous studies, we conjecture that the chain link C_p serves as an ancestor of the 3-manifold at infinity for the critical complex hyperbolic triangle group $\Delta_{p,q,r;\infty}$, where $3 \leq p \leq 9$.

2020 Mathematics Subject Classification: 20H10 (Primary);
57M50, 22E40, 51M10 (Secondary)

1. *Introduction*

1·1. *Motivation*

The relationship between the topology of a manifold and the geometry it admits is a classical topic. For example, Thurston's work on 3-manifolds has shown that geometry plays an important role in the study of the topology of 3-manifolds.

A *spherical CR-structure* on a 3-manifold M is a maximal atlas of charts modeled on the boundary $\partial\mathbf{H}^2_{\mathbb{C}}$ of the complex hyperbolic plane $\mathbf{H}^2_{\mathbb{C}}$, where the transition maps are elements of $\mathbf{PU}(2,1)$. In other words, a *spherical CR-structure* is a (G,X)-structure with $G = \mathbf{PU}(2,1)$ and $X = S^3$. In general, it is difficult to determine whether a 3-manifold admits a spherical

© The Author(s), 2026. Published by Cambridge University Press on behalf of The Cambridge Philosophical Society.

https://doi.org/10.1017/S0305004126102163 Published online by Cambridge University Press

CR-structure. In contrast to other geometric structures admitted by 3-manifolds, there are relatively few known examples admitting spherical CR-structures.

We focus on the following important class: a spherical CR-structure on M is called *uniformisable* if $M = \Gamma\backslash\Omega_\Gamma$, where $\Omega_\Gamma \subset \partial\mathbf{H}^2_{\mathbb{C}}$ is the discontinuity region of a discrete subgroup $\Gamma < \mathbf{PU}(2,1)$ acting on $\partial\mathbf{H}^2_{\mathbb{C}} = S^3$. Thus, the study of discrete subgroups of $\mathbf{PU}(2,1)$ is crucial to understanding uniformisable spherical CR-structures. Complex hyperbolic triangle groups provide rich examples of such discrete subgroups.

Let $T_{p,q,r}$ be the abstract reflection triangle group with the presentation

$$\langle \sigma_1, \sigma_2, \sigma_3 | \sigma_1^2 = \sigma_2^2 = \sigma_3^2 = (\sigma_2\sigma_3)^p = (\sigma_3\sigma_1)^q = (\sigma_1\sigma_2)^r = id \rangle,$$

where each of p, q, r is either a positive integer or ∞ and $1/p + 1/q + 1/r < 1$. One can assume that $p \le q \le r$. If any of p, q, r is equal to ∞, then the corresponding relation is omitted. The ideal triangle group is one with $p = q = r = \infty$. A (p, q, r)-*complex hyperbolic triangle group* is a representation $\rho : T_{p,q,r} \longrightarrow \mathbf{PU}(2,1)$ where the image of each generator is a complex reflection that fixes a complex line. It is well known [21] that the space of (p, q, r)-complex hyperbolic triangle groups has real dimension one when $3 \le p \le q \le r$. Therefore, one can parameterise the family of complex hyperbolic triangle groups by $\rho_t : T_{p,q,r} \to \mathbf{PU}(2,1)$ for $t \in [0,1]$. Here ρ_0 corresponds to the $\mathbb{R}$-Fuchsian case, that is, $\rho_0(T_{p,q,r})$ stabilises an $\mathbb{R}$-plane in $\mathbf{H}^2_{\mathbb{C}}$. We denote the image group of a (p, q, r)-complex hyperbolic triangle group by $\Delta_{p,q,r}$, and set $\rho_t(\sigma_i) = I_i$. We further denote the image group by $\Delta_{p,q,r;\infty}$ when $I_1I_3I_2I_3$ is parabolic.

Goldman and Parker first discussed the complex hyperbolic deformation of the ideal triangle group in [10]. They gave an interval in the moduli space of complex hyperbolic ideal triangle groups whose points correspond to discrete and faithful representations. They conjectured that a complex hyperbolic ideal triangle group $\Delta_{\infty,\infty,\infty} = \langle I_1, I_2, I_3 \rangle$ is discrete and faithful if and only if $I_1I_2I_3$ is not elliptic. Schwartz proved Goldman-Parker's conjecture in [23, 24]. Furthermore, Schwartz [25] analysed the complex hyperbolic ideal triangle group G when $I_1I_2I_3$ is parabolic, and showed that the 3-manifold at infinity of the quotient space $\mathbf{H}^2_{\mathbb{C}}/G$ is commensurable with the Whitehead link complement in the 3-sphere. In particular, the Whitehead link complement admits a uniformisable spherical CR-structure.

In general, for $\Delta_{p,q,r} = \rho_t(T_{p,q,r})$ with $\rho_t(\sigma_i) = I_i$, set

$$W_A = I_1I_3I_2I_3 \quad \text{and} \quad W_B = I_1I_2I_3.$$

Schwartz has also conjectured the following.

CONJECTURE 1·1 (Schwartz [26]). *The set of $t \in [0,1]$ for which ρ_t is a discrete and faithful representation of $T_{p,q,r}$ is the closed interval consisting of the parameters t for which neither W_A nor W_B is elliptic.*

The interval in this conjecture is called the *critical interval*. The non-zero end-point of the critical interval is called the *critical point*. The group $T_{p,q,r}$ is of *type A* if W_A is parabolic in the representation that corresponds to the critical point. This means that W_A becomes elliptic before W_B in the moduli space. Otherwise, we say the group $T_{p,q,r}$ is of *type B*. In particular, $T_{p,q,r}$ is of type A if $p \le 9$ and of type B if $p \ge 14$ [26]. Schwartz's conjecture has been proved in a few cases [19, 20].

The representation at the critical point is particularly interesting. Note that there is a unique $\mathbb{Z}_3$-covering of the Whitehead link complement with four cusps; we denote this

https://doi.org/10.1017/S0305004126102163 Published online by Cambridge University Press

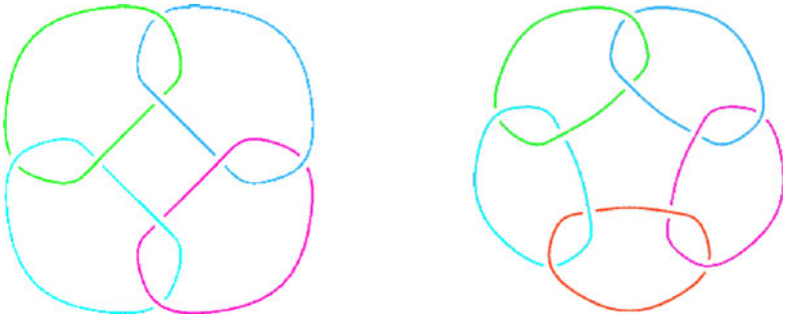


Figure 1. The chain links 8_1^4 (the left) and 10_1^5 (the right). Link diagrams from https://knotinfo.math.indiana.edu/.

manifold by W. If p, q, r are all large enough, then $T_{p,q,r}$ is of type B. Moreover, Schwartz [**27**] showed that the 3-manifold at infinity of the even subgroup of $\Delta_{p,q,r}$ at the critical point is homeomorphic to a manifold obtained by Dehn filling on W. However, for a general critical complex hyperbolic triangle group $\Delta_{p,q,r;\infty}$ of type A, the 3-manifold at infinity of it has not been identified yet. Nevertheless, several explicit examples of cusped hyperbolic 3-manifolds admitting uniformisable spherical CR-structures at these critical representations have been found [**1, 4, 3, 12, 13, 14**]. The construction of these examples typically relies on sophisticated analysis. The underlying topological or geometric reason for the specific identities of these 3-manifolds at infinity remains unclear. Falbel, Guilloux and Will [**8**] proposed the philosophy of predicting the 3-manifold when there is an accidental parabolic element. See [**15**] for the demonstration in a special case. With the main result and conjectures in Section 6, this paper appears to be the initial step in understanding all the 3-manifolds at infinity of complex hyperbolic triangle groups $\Delta_{p,q,r;\infty}$ of type A.

1·2. *Main result of the paper*

The complex hyperbolic triangle group $\Gamma = \Delta_{4,\infty,\infty;\infty}$ acting on the complex hyperbolic plane $\mathbf{H}^2_{\mathbb{C}}$ is generated by complex reflections I_1, I_2, I_3 such that the product I_2I_3 has order four, the products I_3I_1, I_1I_2 are parabolic and the product $I_1I_3I_2I_3$ is an accidental parabolic element. Unexpectedly, the product $I_1I_2I_3I_2$ is a hidden accidental parabolic element. In this paper, we prove the following.

THEOREM 1·2. *Let $\Gamma = \langle I_1, I_2, I_3\rangle$ be the critical complex hyperbolic triangle group $\Delta_{4,\infty,\infty;\infty}$. Then the 3-manifold M at infinity of the even subgroup $\langle I_1I_2, I_2I_3\rangle$ of Γ is the quartic cusped hyperbolic 3-manifold $S^3 - 8_1^4$, where 8_1^4 is the chain link with four components as in Figure 1.*

The link 8_1^4 in Rolfsen's list [**22**] is the first link that has crossing number eight and four components. In Hoste–Thistlethwaite's table, 8_1^4 is also the link $L8a21$.

Let $A = I_1I_2 \in \Delta_{4,\infty,\infty;\infty}$ be a parabolic element fixing a point at infinity. We will prove Theorem 1·2 by studying the Ford domain D_Σ of the even subgroup Σ of $\Delta_{4,\infty,\infty;\infty}$. The topology of the boundary at infinity $\partial_\infty D_\Sigma$ is more complicated than in previous studies [**5, 12, 13, 20**]. One reason is that the boundary of $\partial_\infty D_\Sigma$ is an infinite genus (singular) surface, but all those in [**5, 12, 13, 20**] are unbounded cylinders. Moreover, even though we know the boundary of $\partial_\infty D_\Sigma$ is an infinite genus surface, it is also highly non-trivial to prove

https://doi.org/10.1017/S0305004126102163 Published online by Cambridge University Press

that $\partial_\infty D_\Sigma$ is an infinite genus handlebody, rather than a more complicated 3-manifold with incompressible boundary.

Key Ideas of the Proof of the Theorem 1·2. Figure 2 indicates that $\partial_\infty D_\Sigma$ should be an infinite genus handlebody, where each "hole" corresponds to a genus of the handlebody $\partial_\infty D_\Sigma$. To rigorously prove that $\partial_\infty D_\Sigma$ is a handlebody, our idea is to introduce a set of A-invariant disks $A^k(E_B \cup E_{B^{-1}})$ for $k \in \mathbb{Z}$, which cap off the "holes" in Figure 2. The disks can be constructed as follows:

(i) first, we choose $\mathbb{C}$-arcs on the spinal spheres such that these arcs are compatible with the side-pairs;

(ii) then we construct embedded disks having these $\mathbb{C}$-arcs as their boundaries.

This construction involves choices; there is no unique way to select the arcs or the disks they bound. However, we make specific choices that satisfy the necessary invariance properties.

Figure 3 is a combinatorial model of Figure 2. Figure 9 is a small part of Figure 3. The disks E_B and $E_{B^{-1}}$ are foliated by affine-arcs, so they are ruled surfaces. The intersections $E_B \cap \partial_\infty D_\Sigma$ and $E_{B^{-1}} \cap \partial_\infty D_\Sigma$ are exactly ∂E_B and $\partial E_{B^{-1}}$, respectively:

(i) E_B is a purple topological quadrilateral in Figure 9;

(ii) $E_{B^{-1}}$ is a red topological quadrilateral in Figure 9.

Figure 5 shows a realistic view of E_B and $E_{B^{-1}}$. We decompose $\partial_\infty D_\Sigma$ using the disk family $A^k(E_B \cup E_{B^{-1}}) : k \in \mathbb{Z}$. The resulting complement, denoted $\mathcal{H}$, is an A-invariant horotube homeomorphic to $(\mathbb{R}^2 \setminus \mathbb{D}^2) \times \mathbb{R}$. Having constructed $\mathcal{H}$, we take a fundamental domain for the $\langle A \rangle$-action on it. The 3-manifold M is obtained by applying the full set of side-pairing identifications from D_Σ to this fundamental domain. This process directly yields a presentation for the fundamental group $\pi_1(M)$, completing the proof of Theorem 1·2.

Due to the abundance of conjugacy classes of parabolic elements in Σ, any fundamental domain for this group is necessarily complicated. For example, a Dirichlet domain D for Σ centered at the fixed point of $I_2 I_3$ has an ideal boundary $\partial_\infty D$ that appears to be a genus-three handlebody. Proving that it is indeed a genus-three handlebody, however, presents significant challenges that are not present in the simpler case of [**3**]. For a Dirichlet domain D of $\Delta_{3,3,4;\infty}$ in [**3**], a key step is to show that $\partial_\infty D$ is a solid torus, that is, a genus one handlebody. Although the proof of Theorem 1·2 is quite involved, we believe that the approach via the Ford domain and the invariant disks offers a clear and effective path to the result.

The fact that there are four, rather than three, cusps of the 3-manifold M at infinity of the even subgroup of $\Delta_{4,\infty,\infty;\infty}$ is unexpected. After we have convinced ourselves of this fact (which is not difficult), we continue to study the 3-manifold M_p at infinity of the even subgroup of the complex hyperbolic triangle group $\Delta_{p,\infty,\infty;\infty}$ for $5 \le p \le 9$. Inspired by Theorem 1·2 and the main result in [**14**], we conjecture that the 3-manifold M_p is the complement of the chain link C_p in the 3-sphere. Moreover, supported by previous results, we conjecture that the chain link C_p serves as an 'ancestor' in the sense that the 3-manifolds at infinity for complex hyperbolic triangle groups $\Delta_{p,q,r;\infty}$ with $3 \le p \le 9$ can be obtained from (the complement of) C_p via Dehn surgery. See Section 6 for details.

https://doi.org/10.1017/S0305004126102163 Published online by Cambridge University Press

In other words, a unified picture of the 3-manifolds at infinity for all type *A* critical complex hyperbolic triangle groups is starting to take shape.

Outline of the paper. In Section 2 we give the well-known background material on the complex hyperbolic plane. In Section 3, we give the combinatorial information of the Ford domain for the group $\Delta_{4,\infty,\infty;\infty}$. In Section 4, we study the topology of the ideal boundary of the Ford domain of $\Delta_{4,\infty,\infty;\infty}$. Based on the results in Sections 3 and 4, we show that the 3-manifold at infinity of the even subgroup of $\Delta_{4,\infty,\infty;\infty}$ is the hyperbolic chain link 8_1^4 in Section 5. Finally, we discuss related topics on 3-manifolds associated with the complex hyperbolic triangle groups with accidental parabolic elements in Section 6.

2. *Background*

The complex hyperbolic plane is a simply connected Kähler manifold with constant holomorphic sectional curvature -1. This section reviews the basic geometry of the complex hyperbolic plane. We also refer the reader to Goldman's book [**9**] for more details.

2·1. *The complex hyperbolic plane*

Consider the Hermitian matrix

$$H = \begin{bmatrix} 0 & 0 & 1 \\ 0 & 1 & 0 \\ 1 & 0 & 0 \end{bmatrix}.$$

The Hermitian form on $\mathbb{C}^3$ associated with H is given by $\langle \mathbf{z}, \mathbf{w} \rangle = \mathbf{w}^* H \mathbf{z}$. This form has signature (2,1). Then $\mathbb{C}^3 \setminus 0$ is the disjoint union of the negative cone V_-, the null cone V_0, and the positive cone V_+, where

$$\begin{aligned} V_- &= \{\mathbf{z} \in \mathbb{C}^3 : \langle \mathbf{z}, \mathbf{z} \rangle < 0\}, \\ V_0 &= \{\mathbf{z} \in \mathbb{C}^3 : \langle \mathbf{z}, \mathbf{z} \rangle = 0\} \setminus \{0\}, \\ V_+ &= \{\mathbf{z} \in \mathbb{C}^3 : \langle \mathbf{z}, \mathbf{z} \rangle > 0\}. \end{aligned}$$

Definition 2·1. Let $P : \mathbb{C}^3 \setminus \{0\} \longrightarrow \mathbb{C}P^2$ be the natural projectivisation. The complex hyperbolic plane $\mathbf{H}^2_{\mathbb{C}}$ is defined to be $P(V_-)$, and its boundary $\partial \mathbf{H}^2_{\mathbb{C}}$ is $P(V_0)$. The Bergman metric on $\mathbf{H}^2_{\mathbb{C}}$ is given by the distance formula

$$\cosh^2\left(\frac{d(u,v)}{2}\right) = \frac{\langle \mathbf{u}, \mathbf{v} \rangle \langle \mathbf{v}, \mathbf{u} \rangle}{\langle \mathbf{u}, \mathbf{u} \rangle \langle \mathbf{v}, \mathbf{v} \rangle}, \tag{2·1}$$

where $\mathbf{u}, \mathbf{v} \in \mathbb{C}^3$ are lifts of u,v. Here d(u,v) is the Bergman distance between two points $u, v \in \mathbf{H}^2_{\mathbb{C}}$.

This model of $\mathbf{H}^2_{\mathbb{C}}$ is also called the *Siegel domain*. Let q_∞ be the point at infinity, and let $(z_1, z_2)^T$ be a point of $\overline{\mathbf{H}^2_{\mathbb{C}}} = \mathbf{H}^2_{\mathbb{C}} \cup \partial \mathbf{H}^2_{\mathbb{C}}$. We use $\mathbf{q}_\infty = (1, 0, 0)^T$ to denote the lift of q_∞, and $(z_1, z_2, 1)^T$ as the standard lift of $(z_1, z_2)^T$.

Let $\mathbf{U}(2,1) = \{A \in \mathbf{GL}(3, \mathbb{C}) \mid A^* H A = H\}$, and $\mathbf{PU}(2,1) = \mathbf{U}(2,1)/\mathbf{U}(1)$. Let ω be a primitive cube root of unity. Then $\mathbf{PU}(2,1) = \mathbf{SU}(2,1)/\langle I, \omega I, \omega^2 I \rangle$, which is the holomorphic isometry group of $\mathbf{H}^2_{\mathbb{C}}$.

Elements of $\mathbf{SU}(2,1)$ fall into three types. An isometry is *loxodromic* if it has exactly two fixed points on $\partial \mathbf{H}^2_{\mathbb{C}}$ and *parabolic* if it has exactly one fixed point on $\partial \mathbf{H}^2_{\mathbb{C}}$. An isometry is

https://doi.org/10.1017/S0305004126102163 Published online by Cambridge University Press

called *elliptic* if it has at least one fixed point in $\mathbf{H}^2_{\mathbb{C}}$. An elliptic element is called *regular elliptic* if it has three distinct eigenvalues, otherwise, it is called *special elliptic*.

The trace of a matrix in $\mathbf{SU}(2,1)$ determines the type of the isometry; see Goldman [9, theorem 6·2·4]. Let $A \in \mathbf{SU}(2,1)$ be a non-identity element with real trace. Then A is elliptic if $-1 \leq \mathrm{tr}(A) < 3$. In particular, if $\mathrm{tr}(A) = -1, 0, 1$, A is elliptic of order 2, 3 and 4, respectively. Moreover, A is *unipotent* if $\mathrm{tr}(A) = 3$.

Let ι be given on the level of homogeneous coordinates by complex conjugation $(z_1, z_2, z_3)^T \longmapsto (\overline{z_1}, \overline{z_2}, \overline{z_3})^T$, which is an anti-holomorphic isometry of $\mathbf{H}^2_{\mathbb{C}}$. Any other anti-holomorphic isometry may be written as the composition of ι and an element of $\mathbf{U}(2,1)$.

2·2. *Totally geodesic submanifolds and complex reflections*

There are several types of totally geodesic submanifolds in $\mathbf{H}^2_{\mathbb{C}}$, classified by their dimension: points (0-dim), real geodesics (1-dim), complex lines (2-dim), Lagrangian planes (2-dim), and the entire space (4-dim). Complex lines are the intersections of projective lines in $\mathbb{C}P^2$ with $\mathbf{H}^2_{\mathbb{C}}$, which are also called complex geodesics. Lagrangian planes are the images of $\mathbf{H}^2_{\mathbb{R}}$ under the action of $\mathbf{PU}(2,1)$. As the Riemannian sectional curvature of $\mathbf{H}^2_{\mathbb{C}}$ is non-constant, there is no totally geodesic hypersurface in $\mathbf{H}^2_{\mathbb{C}}$.

The ideal boundary in $\partial\mathbf{H}^2_{\mathbb{C}}$ of a complex line is called a $\mathbb{C}$-circle, and that of a Lagrangian plane is called an $\mathbb{R}$-circle. Let C be a complex line. A *polar vector* of C is the unique positive vector up to scalar multiplication, perpendicular to C with respect to the Hermitian form. Each positive vector corresponds to a complex line.

There is a special class of elliptic elements of order two in $\mathbf{PU}(2,1)$ related to complex lines.

Definition 2·2. The complex reflection on a complex line C with polar vector $\mathbf{n}$ is a holomorphic isometry of order 2, fixing C pointwise, defined by:

$$I_C(\mathbf{z}) = -\mathbf{z} + \frac{2\langle \mathbf{z}, \mathbf{n}\rangle}{\langle \mathbf{n}, \mathbf{n}\rangle}\mathbf{n}. \tag{2·2}$$

The complex line C is usually called the mirror of I_C.

2·3. *The Heisenberg group*

Let $\mathcal{N} = \mathbb{C} \times \mathbb{R}$ be the *Heisenberg group* with product

$$(z, t) \cdot (\zeta, v) = (z + \zeta, t + v + 2\Im(z\bar{\zeta})).$$

Then $\overline{\mathbf{H}^2_{\mathbb{C}}}$ can be identified with $\mathcal{N} \times \mathbb{R}_{\geq 0} \cup \{q_\infty\}$. Any point $q = (z, t, u) \in \mathcal{N} \times \mathbb{R}_{\geq 0}$ has the standard lift

$$\mathbf{q} = \begin{bmatrix} \frac{-|z|^2 - u + it}{2} \\ z \\ 1 \end{bmatrix}.$$

Here (z, t, u) is called the *horospherical coordinates* of $\overline{\mathbf{H}^2_{\mathbb{C}}}$.

https://doi.org/10.1017/S0305004126102163 Published online by Cambridge University Press

When $u=0$, the points are on $\partial\mathbf{H}^2_{\mathbb{C}}$. Hence, we directly identify $\partial\mathbf{H}^2_{\mathbb{C}}$ with the union $\mathcal{N}\cup\{q_\infty\}$. Fixed $u_0>0$, the level set $u=u_0$ is called the *horosphere* based at q_∞, and the sup-level set $u\geq u_0$ is called the *horoball* based at q_∞.

The full stabiliser of $\mathbf{q}_\infty$ is generated by the isometries of the forms

$$T_{[z,t]}=\begin{bmatrix}1 & -\bar{z} & \frac{-|z|^2+it}{2}\\ 0 & 1 & z\\ 0 & 0 & 1\end{bmatrix},\ R_\theta=\begin{bmatrix}1 & 0 & 0\\ 0 & e^{i\theta} & 0\\ 0 & 0 & 1\end{bmatrix}\text{ and }D_\lambda=\begin{bmatrix}\lambda & 0 & 0\\ 0 & 1 & 0\\ 0 & 0 & 1/\lambda\end{bmatrix},$$

where $[z,t]\in\mathcal{N}$, $\theta,\lambda\in\mathbb{R}$ and $\lambda\neq 0$. They are called *Heisenberg translation*, *Heisenberg rotation* and *Heisenberg dilation*, respectively. Their actions on $\mathcal{N}$ are as follows:

$$\begin{aligned}T_{(z,t)}&:(\zeta,v)\longmapsto(z+\zeta,t+v+2\mathrm{Im}(z\bar{\zeta}));\\ R_\theta&:(\zeta,v)\longmapsto(e^{i\theta}\zeta,v);\\ D_\lambda&:(\zeta,v)\longmapsto(\lambda\zeta,\lambda^2 v).\end{aligned}$$

The *Cygan metric* on $\mathcal{N}$ for $p=(z,t)$ and $q=(w,s)\in\mathcal{N}$ is defined by:

$$d_{\mathrm{Cyg}}(p,q)=|2\langle\mathbf{p},\mathbf{q}\rangle|^{1/2}=||z-w|^2-i(t-s+2\Im(z\bar{w}))|^{1/2}. \tag{2·3}$$

In fact, it is the restriction to $\mathcal{N}$ of the *extended Cygan metric*, defined for $p=(z,t,u)$ and $q=(w,s,v)\in\mathcal{N}\times\mathbb{R}_{\geq 0}$ by the formula

$$d_{\mathrm{Cyg}}(p,q)=||z-w|^2+|u-v|-i(t-s+2\Im(z\bar{w}))|^{1/2}. \tag{2·4}$$

The *Cygan sphere* with center $(z_0,t_0)\in\mathcal{N}$ and radius $r>0$ in $\overline{\mathbf{H}^2_{\mathbb{C}}}$, is defined by

$$S_{[z_0,t_0]}(r)=\left\{(z,t,u)\in\overline{\mathbf{H}^2_{\mathbb{C}}}:\left||z-z_0|^2+u+i(t-t_0+2\Im(z\overline{z_0}))\right|=r^2\right\}. \tag{2·5}$$

Note that $S_{[z_0,t_0]}(r)$ can be obtained by the action of $T_{[z_0,t_0]}$ on $S_{[0,0]}(r)$. There is another way to define a Cygan sphere:

Definition 2·3. The geographic coordinates (α,β,w) of $q=q(\alpha,\beta,w)\in S_{[0,0]}(r)$ is given by the lift

$$\mathbf{q}=\mathbf{q}(\alpha,\beta,w)=\begin{bmatrix}-r^2e^{-i\alpha}/2\\ rwe^{i(-\alpha/2+\beta)}\\ 1\end{bmatrix}, \tag{2·6}$$

where $\alpha\in[-\pi/2,\pi/2]$, $\beta\in[0,\pi)$ and $w\in[-\sqrt{\cos(\alpha)},\sqrt{\cos(\alpha)}]$. In particular, the ideal boundary of $S_{[0,0]}(r)$ on $\partial\mathbf{H}^2_{\mathbb{C}}$ are the points with $w=\pm\sqrt{\cos(\alpha)}$.

The following proposition describes the characteristics of the level sets for α and β.

PROPOSITION 2·4 (Goldman [9], Parker and Will [20]). *Let $S_{[0,0]}(r)$ be a Cygan sphere with geographic coordinates (α,β,w).*

(i) *For each $\alpha_0\in[-\pi/2,\pi/2]$, the set of points in $S_{[0,0]}(r)$ with $\alpha=\alpha_0$ is a complex line, called a slice of $S_{[0,0]}(r)$.*

https://doi.org/10.1017/S0305004126102163 Published online by Cambridge University Press

(ii) *For each $\beta_0 \in [0, \pi)$, the set of points in $S_{[0,0]}(r)$ with $\beta = \beta_0$ is a Lagrangian plane, called a meridian of $S_{[0,0]}(r)$.*

(iii) *The set of points with $w = 0$ is called the real spine of $S_{[0,0]}(r)$.*

Regarding the intersection of Cygan spheres, Goldman, Parker and Will proved the following result.

PROPOSITION 2·5 (Goldman [9], Parker and Will [20]). *The intersection of two Cygan spheres is a smooth disk.*

Remark 2·6. This disk is frequently called a Giraud disk.

2·4. *Isometric spheres and Ford polyhedron*

Let $g = (g_{ij})$ be an element of $\mathbf{PU}(2, 1)$ not fixing $\mathbf{q}_\infty$. This implies that $g_{31} \neq 0$.

Definition 2·7. The isometric sphere of g, denoted by I(g), is the set

$$I(g) = \left\{ p \in \overline{\mathbf{H}^2_{\mathbb{C}}} : |\langle \mathbf{p}, \mathbf{q}_\infty \rangle| = |\langle \mathbf{p}, g^{-1}(\mathbf{q}_\infty) \rangle| \right\}. \tag{2·7}$$

An isometric sphere is a 3-ball. The *spinal sphere* of $I(g)$ or g is defined to be $I(g) \cap \partial \mathbf{H}^2_{\mathbb{C}}$, denoted by $\partial_\infty I(g)$, which is a 2-sphere. Besides, $I(g)$ is exactly the Cygan sphere with center $g^{-1}(\mathbf{q}_\infty) \in \mathcal{N}$ and radius $r_g = \sqrt{2/|g_{31}|}$. The *interior* of $I(g)$ is the set

$$\left\{ p \in \overline{\mathbf{H}^2_{\mathbb{C}}} : |\langle \mathbf{p}, \mathbf{q}_\infty \rangle| > |\langle \mathbf{p}, g^{-1}(\mathbf{q}_\infty) \rangle| \right\}. \tag{2·8}$$

The *exterior* of $I(g)$ is the set

$$\left\{ p \in \overline{\mathbf{H}^2_{\mathbb{C}}} : |\langle \mathbf{p}, \mathbf{q}_\infty \rangle| < |\langle \mathbf{p}, g^{-1}(\mathbf{q}_\infty) \rangle| \right\}. \tag{2·9}$$

We summarise some properties on isometric spheres in the following proposition.

PROPOSITION 2·8 ([9, section 5·4·5]). *Let g and h be elements of $\mathbf{PU}(2, 1)$ which do not fix $\mathbf{q}_\infty$ and $g^{-1}(\mathbf{q}_\infty) \neq h^{-1}(\mathbf{q}_\infty)$. Let $f \in \mathbf{PU}(2, 1)$ be a unipotent map fixing $\mathbf{q}_\infty$. Then the following hold*:

(i) *$g(I(g)) = I(g^{-1})$, and g maps the exterior of $I(g)$ to the interior of $I(g^{-1})$;*

(ii) *$I(gf) = f^{-1}I(g)$, $I(fg) = I(g)$;*

(iii) *$g(I(g) \cap I(h)) = I(g^{-1}) \cup I(hg^{-1})$, $h(I(g) \cap I(h)) = I(gh^{-1}) \cup I(h^{-1})$.*

Definition 2·9. The Ford domain D_Γ for a discrete group $\Gamma < \mathbf{PU}(2, 1)$ centred at q_∞ is the intersection of the closures of the exteriors of all isometric spheres of elements in Γ not fixing $\mathbf{q}_\infty$. That is,

$$D_\Gamma = \left\{ p \in \overline{\mathbf{H}^2_{\mathbb{C}}} : |\langle \mathbf{p}, \mathbf{q}_\infty \rangle| \leq |\langle \mathbf{p}, g^{-1}(\mathbf{q}_\infty) \rangle| \ \forall g \in \Gamma \text{ with } g(\mathbf{q}_\infty) \neq \mathbf{q}_\infty \right\}.$$

The boundary at infinity of the Ford domain is made up of pieces of isometric spheres. When q_∞ is in the domain of discontinuity or is a parabolic fixed point, the Ford domain is preserved by Γ_∞, the stabiliser of q_∞ in Γ. In this case, the fundamental domain for Γ is

https://doi.org/10.1017/S0305004126102163 Published online by Cambridge University Press

the intersection of D_Γ with a fundamental domain for Γ_∞. Facets of codimensions one, two, three and four in D_Γ are called *sides*, *ridges*, *edges* and *vertices*, respectively. Moreover, a *bounded ridge* is a ridge that does not intersect $\partial\mathbf{H}^2_{\mathbb{C}}$. Otherwise, the ridge is called an *infinite ridge*.

It is usually very hard to determine the Ford domain D_Γ because one should check infinitely many inequalities. A common approach is to propose a candidate for the Ford polyhedron and then verify it using the Poincaré polyhedron theorem. The sides of D_Γ should be paired by isometries, and the images of D_Γ under these so-called side-pairing maps should give a local tiling of $\mathbf{H}^2_{\mathbb{C}}$. If they do, and if, moreover, the quotient of D_Γ by the identification given by the side-pairing maps is complete, the Poincaré polyhedron theorem implies that the images of D_Γ give a global tiling of $\mathbf{H}^2_{\mathbb{C}}$.

Once a fundamental domain is obtained, one gets a presentation of Γ. Its generators are given by the side-pairing maps together with a generating set of Γ_∞. Its relations come from ridge cycles, which correspond to the local tilings around each codimension-two face. For more details on the Poincaré polyhedron theorem, see [**6, 20**].

3. *Combinatoric of Ford domain of* $\Delta_{4,\infty,\infty;\infty}$

In this section, we study the combinatorics of the Ford domain of $\Delta_{4,\infty,\infty;\infty}$. The main result is Theorem 3·6.

3·1. *The matrix representation of the triangle group* $\Delta_{4,\infty,\infty;\infty}$

Suppose J_1 and J_2 are two complex reflections in $\mathbf{SU}(2,1)$ such that J_1J_2 is a unipotent map fixing q_∞. Conjugating by a Heisenberg rotation and a Heisenberg dilation if necessary, we may suppose that J_1 and J_2 are

$$J_1 = \begin{bmatrix} -1 & 0 & 0 \\ 0 & 1 & 0 \\ 0 & 0 & -1 \end{bmatrix}, \quad J_2 = \begin{bmatrix} -1 & -2 & 2 \\ 0 & 1 & -2 \\ 0 & 0 & -1 \end{bmatrix}. \tag{3·1}$$

We want to find J_3 such that J_2J_3 is an elliptic element of order 4, and J_3J_1, J_1J_2, $J_1J_3J_2J_3$ are unipotent. Assume that the polar vector of the mirror of J_3 is

$$\mathbf{n}_3 = \begin{bmatrix} x \\ y + zi \\ 1 \end{bmatrix},$$

where $x, y, z \in \mathbb{R}$. Then J_3 has the following form

$$J_3 = \begin{bmatrix} \dfrac{-y^2 - z^2}{y^2 + z^2 + 2x} & \dfrac{2x(y - zi)}{y^2 + z^2 + 2x} & \dfrac{2x^2}{y^2 + z^2 + 2x} \\ \dfrac{2(y + zi)}{y^2 + z^2 + 2x} & \dfrac{y^2 + z^2 - 2x}{y^2 + z^2 + 2x} & \dfrac{2x(y + zi)}{y^2 + z^2 + 2x} \\ \dfrac{2}{y^2 + z^2 + 2x} & \dfrac{2(y - zi)}{y^2 + z^2 + 2x} & \dfrac{-y^2 - z^2}{y^2 + z^2 + 2x} \end{bmatrix}.$$

Note that J_3J_1 is unipotent, which implies that its trace is 3, yielding $x = 0$. Similarly, since J_1J_2 and $J_1J_3J_2J_3$ are unipotent, we have $y = 1$ and $z = \pm 1$. The groups corresponding to

https://doi.org/10.1017/S0305004126102163 Published online by Cambridge University Press

$z = \pm 1$ are conjugate via an anti-holomorphic isometry. In this paper, we take $z = 1$, then

$$J_3 = \begin{bmatrix} -1 & 0 & 0 \\ 1+i & 1 & 0 \\ 1 & 1-i & -1 \end{bmatrix}.$$

Moreover, $\langle J_1, J_2, J_3 \rangle$ is an infinite-index subgroup of the Gauss-Picard modular group $\mathbf{PU}(2, 1; \mathbb{Z}[i])$, proving that $\langle J_1, J_2, J_3 \rangle$ is discrete; see [7]. We thank the referee for pointing out that our results may be derived from the Ford domain of the Gauss-Picard modular group. The discreteness of $\Delta_{4,\infty,\infty;\infty}$ was first noted by Thompson [28].

For technical reasons, we conjugate the matrix representation of $\Delta_{4,\infty,\infty;\infty}$ by

$$T = \begin{bmatrix} 1 & 1 & \frac{-1-2i}{2} \\ 0 & 1 & -1 \\ 0 & 0 & 1 \end{bmatrix}.$$

That is, let $I_1 = TJ_1T^{-1}$, $I_2 = TJ_2T^{-1}$, and $I_3 = TJ_3T^{-1}$ be generators of $\Delta_{4,\infty,\infty;\infty}$. Specifically:

$$I_1 = \begin{bmatrix} -1 & 2 & 2 \\ 0 & 1 & 2 \\ 0 & 0 & -1 \end{bmatrix}, \quad I_2 = \begin{bmatrix} -1 & 0 & 0 \\ 0 & 1 & 0 \\ 0 & 0 & -1 \end{bmatrix}, \quad I_3 = \begin{bmatrix} -1/2 & -i/2 & 1/4 \\ i & 0 & i/2 \\ 1 & -i & -1/2 \end{bmatrix}. \quad (3{\cdot}2)$$

3·2. *Ford domain of* $\Delta_{4,\infty,\infty;\infty}$

Let $\Gamma = \langle I_1, I_2, I_3 \rangle$ be the group $\Delta_{4,\infty,\infty;\infty}$. Let $A = I_1I_2$, $B = I_2I_3$. The subgroup generated by A and B, denoted by $\Sigma = \langle A, B \rangle$, is the even subgroup of Γ with index two. By direct calculation, we have the following.

$$A = \begin{bmatrix} 1 & 2 & -2 \\ 0 & 1 & -2 \\ 0 & 0 & 1 \end{bmatrix}, \quad B = \begin{bmatrix} \frac{1}{2} & \frac{i}{2} & -\frac{1}{4} \\ i & 0 & \frac{i}{2} \\ -1 & i & \frac{1}{2} \end{bmatrix}.$$

Due to the definition of $\Delta_{4,\infty,\infty;\infty}$, we have that B is elliptic of order 4, and there are three unipotent elements, A, AB, and AB^2. In addition, AB^{-1} is also unipotent. For future reference, we provide the lifts of their fixed points, as vectors in $\mathbb{C}^3$:

$$\mathbf{p}_{AB} = x_1 = \begin{bmatrix} -\frac{1+2i}{2} \\ -1 \\ 1 \end{bmatrix}, \ \mathbf{p}_{AB^2} = x_2 = \begin{bmatrix} -\frac{1}{2} \\ -1 \\ 1 \end{bmatrix} \text{ and } \mathbf{p}_{AB^{-1}} = x_3 = \begin{bmatrix} \frac{-1+2i}{2} \\ -1 \\ 1 \end{bmatrix}$$

In this subsection, we will construct a Ford domain D_Σ whose sides are contained in the isometric spheres of some elements of Σ. The reader is referred to Figures 2 and 3 for visualisations of D_Σ. Figure 2 provides a realistic depiction of the ideal boundary of D_Σ, centered at q_∞, for motivational purposes. In this subsection, we will verify that the local combinatorial structure matches this figure.

In Figure 2:

(i) the green, black and red spheres are the spinal spheres of $A^{-1}BA$, B and ABA^{-1}, respectively;

https://doi.org/10.1017/S0305004126102163 Published online by Cambridge University Press

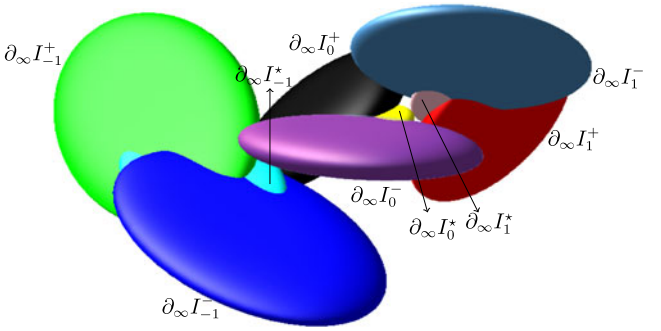


Figure 2. A realistic view the ideal boundary of the Ford domain of $\Delta(4,\infty,\infty;\infty)$.

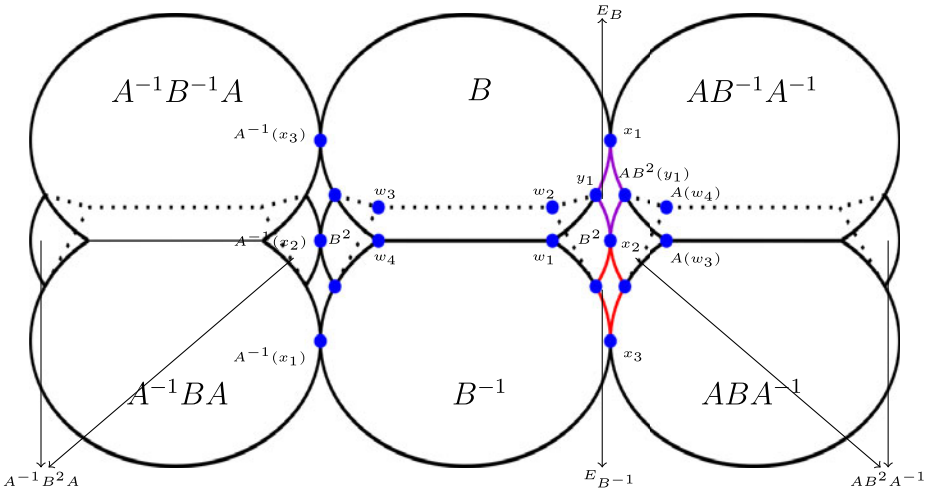


Figure 3. An abstract picture of the Ford domain of Σ. For example, the sphere labelled by B is the spinal sphere $\partial_\infty I(B)$, in the notation of Proposition 3·4, it is $\partial_\infty I^+_0$.

(ii) the blue, purple and steel-blue spheres are the spinal spheres of $A^{-1}B^{-1}A$, B^{-1} and $AB^{-1}A^{-1}$, respectively;

(iii) the cyan, yellow and pink spheres are the spinal spheres of $A^{-1}B^2A$, B^2 and AB^2A^{-1} respectively.

Figure 3 is a combinatorial model of Figure 2. Our subsequent computations will show that the combinatorial model is consistent with Figure 2.

Let $I(B)$, $I(B^{-1})$ and $I(B^2)$ be the isometric spheres for B, B^{-1} and B^2, respectively. We give some notation for the isometric spheres, which are the images of $I(B)$, $I(B^{-1})$, and $I(B^2)$ by powers of A.

Definition 3·1. For $k \in \mathbb{Z}$:

(1) Let I^+_k be the isometric sphere $I(A^kBA^{-k}) = A^kI(B)$ and $\partial_\infty I^+_k$ be its corresponding spinal sphere;

https://doi.org/10.1017/S0305004126102163 Published online by Cambridge University Press

(2) Let I_k^- be the isometric sphere $I(A^kB^{-1}A^{-k}) = A^kI(B^{-1})$ and $\partial_\infty I_k^-$ be its corresponding spinal sphere;

(3) Let $I_k^\star$ be the isometric sphere $I(A^kB^2A^{-k}) = A^kI(B^2)$ and $\partial_\infty I_k^*$ be its corresponding spinal sphere.

The action of A on $\mathcal{N}$ is given by

$$(z, t) \longmapsto (z - 2, t + 4\Im(z)). \tag{3·3}$$

In particular, we have the following.

PROPOSITION 3·2. *For any value of $t_0 \in \mathbb{R}$, A preserves every $\mathbb{R}$-circle of the form (x, t_0) with $x \in \mathbb{R}$.*

As A is unipotent and fixes q_∞, it is a Cygan isometry and preserves the radii of the isometric spheres. This directly proves

PROPOSITION 3·3. *For any integer $k \in \mathbb{Z}$:*

(i) *the isometric spheres I_k^+ and I_k^- have the same radius $\sqrt{2}$ and are centered at $(-2k + i, -4k)$ and $(-2k - i, 4k)$ in Heisenberg coordinates, respectively;*

(ii) *the isometric sphere $I_k^\star$ has a radius 1 and is centered at $(-2k, 0)$ in Heisenberg coordinates.*

We first consider the intersections of the isometric spheres $I_k^\pm$ and $I_k^\star$ for $k \in \mathbb{Z}$. By the A-symmetry, $I_l^+ \cap I_{l+k}^+$ is non-empty if and only if $I_0^+ \cap I_k^+$ is non-empty. Similar properties hold for other intersections of pairs of isometric spheres.

PROPOSITION 3·4. *For any $k \in \mathbb{Z}$:*

(i) *I_0^+ is disjoint from I_k^+ when $|k| \geq 2$;*

(ii) *I_0^- is disjoint from I_k^- when $|k| \geq 2$;*

(iii) *I_0^+ is disjoint from I_k^- when $k \neq 0$;*

(iv) *$I_0^\star$ is disjoint from $I_k^\star$ when $|k| \geq 2$;*

(v) *$I_0^\star$ is disjoint from $I_k^\pm$ when $|k| \geq 1$;*

(vi) *I_0^+ is tangent to I_1^- at the point x_1;*

(vii) *I_0^- is tangent to I_1^+ at the point x_3;*

(viii) *$I_0^\star$ is tangent to $I_1^\star$ at the point x_2.*

Proof. The assertion (i) follows from the fact that the Cygan distance between the centers of I_0^+ and I_k^+ is $|2k|$, which is greater than $2\sqrt{2}$ when $|k| \geq 2$. Similarly, we have the assertion (ii).

For (iii), the Cygan distance between the centers of I_0^+ and I_k^- is $2\sqrt{k^2 + 1}$, which is greater than $2\sqrt{2}$ when $|k| \geq 2$. Hence, I_0^+ is disjoint from I_k^- if $|k| \geq 2$. When $k = \pm 1$, we assume that

$$(x + yi, t) \in \partial_\infty I_0^+ \cap \partial_\infty I_{\pm 1}^-$$

https://doi.org/10.1017/S0305004126102163 Published online by Cambridge University Press

in Heisenberg coordinates with $x, y, t \in \mathbb{R}$. Then considering the equation of an isometric sphere in the Definition 2·7, it is easy to show that there is no $(x + yi, t)$ lying in $\partial_\infty I_0^+ \cap \partial_\infty I_{\pm 1}^-$. This implies that $I_0^+ \cap I_{\pm 1}^- = \emptyset$.

The assertion (iv) follows from the fact that the Cygan distance between the centers of $I_0^\star$ and $I_k^\star$ is $|2k|$, which is greater than 2 when $|k| \geq 2$. The assertion (v) follows from the fact that the Cygan distance between the centers of $I_0^\star$ and $I_k^\pm$ is $\sqrt{16k^4 + 24k^2 + 1}$, which is greater than $\sqrt{2} + 1$ when $|k| \geq 1$.

For a unipotent element $g \in \mathbf{PU}(2, 1)$, the isometric spheres $I(g)$ and $I(g^{-1})$ are tangent, where the tangent point is exactly the fixed point of g. The assertions (vi), (vii), (viii) follow from the fact that AB, AB^{-1} and AB^2 are unipotent.

Definition 3·5. The infinite polyhedron D_Σ is the intersection of the exteriors of all the isometric spheres in $\{I_k^+, I_k^-, I_k^\star : k \in \mathbb{Z}\}$. That is,

$$D_\Sigma = \{p \in \mathbf{H}^2_{\mathbb{C}} : |\langle \mathbf{p}, \mathbf{q}_\infty \rangle| \leq |\langle \mathbf{p}, A^k B^i(\mathbf{q}_\infty) \rangle|, \forall k \in \mathbb{Z} \text{ and } i = 1, 2, 3\}.$$

We shall use a version of the Poincaré polyhedron theorem for coset decompositions because D_Σ is stabilised by the cyclic subgroup $\langle A \rangle$. See [**6, 20**] for the precise statement of this version of the Poincaré polyhedron theorem. We proceed to show:

THEOREM 3·6. *The polyhedron D_Σ is a fundamental domain for the cosets of $\langle A \rangle$ in $\Sigma = \langle A, B \rangle$. Moreover, the group Σ is discrete and has the presentation*

$$\langle A, B : B^4 = id \rangle.$$

For any $k \in \mathbb{Z}$, we denote $I_k^+ \cap D_\Sigma$, $I_k^- \cap D_\Sigma$, and $I_k^\star \cap D_\Sigma$ by s_k^+, s_k^-, and $s_k^\star$, respectively. We will show that they are 3-faces of D_Σ. Let

$$w_1 = \begin{bmatrix} -\frac{1+2\sqrt{2}i}{6} \\ -\frac{\sqrt{2}+i}{3} \\ 1 \end{bmatrix}, w_2 = \begin{bmatrix} -\frac{1-2\sqrt{2}i}{6} \\ -\frac{\sqrt{2}-i}{3} \\ 1 \end{bmatrix}, w_3 = \begin{bmatrix} -\frac{1-2\sqrt{2}i}{6} \\ \frac{\sqrt{2}-i}{3} \\ 1 \end{bmatrix} \text{ and } w_4 = \begin{bmatrix} -\frac{1+2\sqrt{2}i}{6} \\ \frac{\sqrt{2}+i}{3} \\ 1 \end{bmatrix}$$

be four points. Moreover, one can verify that $B(w_1) = w_4$, $B(w_4) = w_3$, $B(w_3) = w_2$, and $B(w_2) = w_1$.

PROPOSITION 3·7. *For the isometric spheres I_0^+, I_0^- and $I_0^\star$:*

(i) *each of $I_0^+ \cap I_0^-$, $I_0^+ \cap I_0^\star$ and $I_0^- \cap I_0^\star$ is a Giraud disk;*

(ii) *the triple intersection $I_0^+ \cap I_0^- \cap I_0^\star$ is a union of two geodesics crossed at the fixed point of B, whose four endpoints are on $\partial \mathbf{H}^2_{\mathbb{C}}$;*

(iii) *the four points w_1, w_2, w_3 and w_4 are exactly the set*

$$I_0^+ \cap I_0^- \cap I_0^\star \cap \partial \mathbf{H}^2_{\mathbb{C}}.$$

Proof. First note that the fixed point of B in $\mathbf{H}^2_{\mathbb{C}}$ is

$$\mathbf{p}_B = \begin{bmatrix} -1/2 \\ 0 \\ 1 \end{bmatrix}.$$

https://doi.org/10.1017/S0305004126102163 Published online by Cambridge University Press

A direct computation shows that $\mathbf{p}_B$ lies in I_0^+, I_0^-, and $I_0^\star$. Moreover, q_∞, $B(q_\infty)$ and $B^2(q_\infty)$ are linearly independent. By Proposition 2·5, $I_0^- \cap I_0^\star$ is a non-empty Giraud disk. Similarly, each of $I_0^+ \cap I_0^-$ and $I_0^+ \cap I_0^\star$ is a non-empty Giraud disk.

We now consider the triple intersection $I_0^+ \cap I_0^- \cap I_0^\star$. From (2.6), the geographic coordinates (α, β, w) of points in $I_0^\star$ are given by

$$\mathbf{q} = \mathbf{q}(\alpha, \beta, w) = \begin{bmatrix} -e^{-i\alpha}/2 \\ we^{i(-\alpha/2+\beta)} \\ 1 \end{bmatrix}, \tag{3·4}$$

where $\alpha \in [-\pi/2, \pi/2]$, $\beta \in [0, \pi)$ and $w \in [-\sqrt{\cos(\alpha)}, \sqrt{\cos(\alpha)}]$. Since $\mathbf{q} \in I_0^\star$, we have

$$|\langle \mathbf{q}, (q_\infty)\rangle|^2 = |\langle \mathbf{q}, B^{-2}(q_\infty)\rangle|^2 = 1.$$

We calculate $|\langle \mathbf{q}, B^{-1}(q_\infty)\rangle|^2$ to be

$$w^2 + \frac{1+\cos(\alpha)}{2} + w\left(\sin\left(\frac{\alpha-2\beta}{2}\right) - \sin\left(\frac{\alpha+2\beta}{2}\right)\right) \tag{3·5}$$

and $|\langle \mathbf{q}, B(q_\infty)\rangle|^2$ to be

$$w^2 + \frac{1+\cos(\alpha)}{2} - w\left(\sin\left(\frac{\alpha-2\beta}{2}\right) - \sin\left(\frac{\alpha+2\beta}{2}\right)\right). \tag{3·6}$$

Then the triple intersection $I_0^+ \cap I_0^- \cap I_0^\star$ is given by

$$\begin{cases} w^2 + \dfrac{1+\cos(\alpha)}{2} = 1; \\ w\left(\sin\left(\dfrac{\alpha-2\beta}{2}\right) - \sin\left(\dfrac{\alpha+2\beta}{2}\right)\right) = 0. \end{cases} \tag{3·7}$$

The solutions are

$$\alpha = \pi, \quad \text{or} \quad w = 0, \quad \text{or} \quad \beta = 0.$$

Since $\alpha \in [-\pi/2, \pi/2]$, we know that $\alpha = \pi$ is not a solution of our equation. If $w = 0$, then $\alpha = 0$, which corresponds to the point $\mathbf{p}_B$. If $\beta = 0$, the solutions lie in a meridian of $I_0^\star$. In this case, the set $\mathbf{q}(\alpha, 0, w)$ is a union of two geodesics which intersect at $\mathbf{p}_B$, where $w = \pm\sqrt{(1-\cos(\alpha))/2}$.

Moreover, in the case of $\beta = 0$, we consider the intersection of $I_0^+ \cap I_0^- \cap I_0^\star$ with $\partial\mathbf{H}^2_{\mathbb{C}}$. Note that $|\langle \mathbf{q}, \mathbf{q}\rangle|^2 = w^2 - \cos(\alpha)$. If $\mathbf{q} \in \partial\mathbf{H}^2_{\mathbb{C}}$, we have $w = \pm\sqrt{\cos(\alpha)}$. Hence the equation $\pm\sqrt{\cos(\alpha)} = \pm\sqrt{(1-\cos(\alpha))/2}$ gives the intersection point. Specifically,

$$\alpha = \pm\arccos\left(\frac{1}{3}\right), \quad \beta = 0, \quad w = \pm\frac{1}{3^{1/2}}.$$

The coordinates of the points w_i for $i = 1, 2, 3, 4$ are as given above.

From Proposition 3·7, we have the following three propositions on the combinatorics of 3-faces s_0^+, s_0^- and $s_0^\star$. The readers are referred to Figure 4 for illustrations.

https://doi.org/10.1017/S0305004126102163 Published online by Cambridge University Press

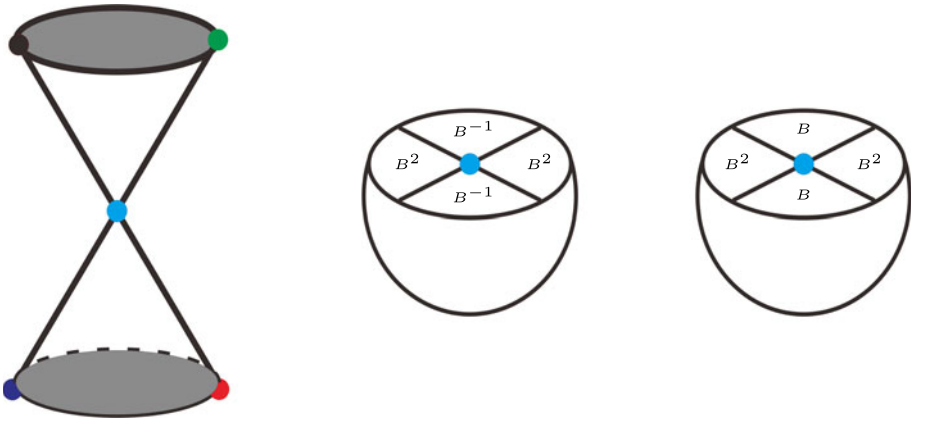


Figure 4. 3-sides of D_Σ. The left one is $s_0^\star$, the two shaded disks are $s_0^\star \cap \partial\mathbf{H}^2_{\mathbb{C}}$. The central one is s_0^+, the B^{-1}-labelled sectors are $s_0^+ \cap s_0^-$, the B^2-labelled sectors are $s_0^+ \cap s_0^\star$. The right one is s_0^-, the labelled sectors have similar meanings. In each sub-figure, the fixed point of B is indicated in cyan (for the online edition) or grey (for the print edition).

PROPOSITION 3·8. *For the 3-face s_0^+ of D_Σ:*

(i) *$s_0^+ \cap s_0^-$ is topologically the union of two sectors;*
(ii) *$s_0^+ \cap s_0^\star$ is topologically the union of two sectors;*
(iii) *$\partial s_0^+ \cap \partial\mathbf{H}^2_{\mathbb{C}}$ is a disk;*
(iv) *s_0^+ is a 3-ball in $\overline{\mathbf{H}^2_{\mathbb{C}}}$, and ∂s_0^+ is the union of $\partial s_0^+ \cap \partial\mathbf{H}^2_{\mathbb{C}}$, $s_0^+ \cap s_0^-$ and $s_0^+ \cap s_0^\star$.*

Proof. The side s_0^+ is contained in the isometric sphere I_0^+. Besides I_0^+ is tangent to I_{-1}^- and I_1^- at a parabolic fixed point respectively, the isometric sphere I_0^+ does not intersect with any other isometric spheres except I_0^- and $I_0^\star$. By Proposition 3·7, both $I_0^+ \cap I_0^-$ and $I_0^+ \cap I_0^\star$ are topologically a union of two sectors. These intersections are glued along $I_0^+ \cap I_0^- \cap I_0^\star$ to form a disk in the boundary of s_0^+. The boundary of this disk bounds a disk in $I_0^+ \cap \mathbf{H}^2_{\mathbb{C}}$. Together, these two disks cobound a 3-ball in I_0^+, which is s_0^+.

The proof of Proposition 3·9 is similar and is omitted.

PROPOSITION 3·9. *For the 3-face s_0^+ of D_Σ:*

(i) *$s_0^- \cap s_0^+$ is topologically the union of two sectors;*
(ii) *$s_0^- \cap s_0^\star$ is topologically the union of two sectors;*
(iii) *$\partial s_0^- \cap \partial\mathbf{H}^2_{\mathbb{C}}$ is a disk;*
(iv) *s_0^- is a 3-ball in $\overline{\mathbf{H}^2_{\mathbb{C}}}$, and ∂s_0^- is the union of $\partial s_0^- \cap \partial\mathbf{H}^2_{\mathbb{C}}$, $s_0^- \cap s_0^+$ and $s_0^- \cap s_0^\star$.*

PROPOSITION 3·10. *For the 3-face $s_0^\star$ of D_Σ:*

(i) *$s_0^\star \cap s_0^+$ is topologically the union of two sectors*;
(ii) *$s_0^\star \cap s_0^-$ is topologically the union of two sectors*;

https://doi.org/10.1017/S0305004126102163 Published online by Cambridge University Press

(iii) $\partial s_\star^- \cap \partial \mathbf{H}^2_{\mathbb{C}}$ *is the union of two disjoint disks*;

(iv) $s_0^\star$ *is a topologically solid light cone in* $\overline{\mathbf{H}^2_{\mathbb{C}}}$, *and* ∂s_0^+ *is the union of* $\partial s_0^+ \cap \partial \mathbf{H}^2_{\mathbb{C}}$, $s_0^\star \cap s_0^-$ *and* $s_0^\star \cap s_0^+$.

Proof. The side $s_0^\star$ is contained in the isometric sphere $I_0^\star$. Besides being tangent to $I_{-1}^\star$ and $I_1^\star$ at parabolic fixed points, the isometric sphere $I_0^\star$ does not intersect any other isometric spheres except I_0^+ and I_0^-. By Proposition 3·7, both $I_0^\star \cap I_0^+$ and $I_0^\star \cap I_0^-$ are topologically a union of two sectors. We also have that $I_0^\star \cap I_0^+$ and $I_0^\star \cap I_0^-$ are glued together along $I_0^+ \cap I_0^- \cap I_0^\star$ to a light cone on the boundary of $s_0^\star$. The boundaries of this light cone are two simple curves. Each of them bounds a disk in $I_0^\star \cap \mathbf{H}^2_{\mathbb{C}}$. The light cone and the two disks together co-bound a topologically solid light cone in $I_0^\star$, which is $s_0^\star$.

The side pairing maps on D_Σ are defined by:

$$A^k B A^{-k} : s_k^+ \longrightarrow s_k^-, \quad A^k B^{-1} A^{-k} : s_k^- \longrightarrow s_k^+, \quad A^k B^2 A^{-k} : s_k^\star \longrightarrow s_k^\star.$$

By the A-symmetry, we may only consider the following properties.

PROPOSITION 3·11. *For the side-pairings* B *and* B^2:

(i) *the side pairing map* B *is a homeomorphism from* s_0^+ *to* s_0^-. *Furthermore,* B *sends the ridge* $s_0^+ \cap s_0^-$ *to* $s_0^- \cap s_0^\star$ *and sends the ridge* $s_0^+ \cap s_0^\star$ *to* $s_0^- \cap s_0^+$;

(ii) *the side pairing map* B^2 *is a self-homeomorphism of* $s_0^\star$, *and it exchanges the ridges* $s_0^+ \cap s_0^\star$ *and* $s_0^- \cap s_0^\star$.

Proof. The ridge $s_0^+ \cap s_0^-$ is defined by the triple equality

$$|\langle z, \mathbf{q}_\infty \rangle| = |\langle z, B^{-1}(\mathbf{q}_\infty) \rangle| = |\langle z, B(\mathbf{q}_\infty) \rangle|.$$

The map B sends

$$\{\mathbf{q}_\infty, B^{-1}(\mathbf{q}_\infty), B(\mathbf{q}_\infty)\}$$

to

$$\{B(\mathbf{q}_\infty), \mathbf{q}_\infty, B^2(\mathbf{q}_\infty)\}.$$

So B sends the ridge $s_0^+ \cap s_0^-$ to $s_0^- \cap s_0^\star$. Another claim in Proposition 3·11 can be proved similarly.

Proof of Theorem 3·6. After Propositions 3·8, 3·9, 3·10 and 3·11.
Local tessellation. We prove the tessellations around the sides and ridges of D_Σ.

(1) Since $A^k B^\pm A^{-k}$ sends the exterior of $I_k^\pm$ to the interior of $I_k^\mp$, we see that D_Σ and $A^k B^\pm A^{-k}(D_\Sigma)$ have disjoint interiors and cover a neighbourhood of each point in the interior of the 3-side $s_k^\mp$.

(2) For the ridge $s_0^+ \cap s_0^\star$, the ridge circle is

$$s_0^+ \cap s_0^\star \xrightarrow{B} s_0^+ \cap s_0^- \xrightarrow{B} s_0^- \cap s_0^\star \xrightarrow{B^2} s_0^+ \cap s_0^\star.$$

This gives the relation $B^4 = id$; By a standard argument as in [**20**], we have that $D_\Sigma \cup B^2(D_\Sigma) \cup B^{-1}(D_\Sigma)$ covers a small neighborhood of $s_0^+ \cap s_0^\star$.

https://doi.org/10.1017/S0305004126102163 Published online by Cambridge University Press

Completeness. We must construct a system of consistent horoballs at the parabolic fixed points. First, we consider the side pairing maps on the parabolic fixed points $x_1 = p_{AB}$, $x_2 = p_{AB^2}$ and $x_3 = p_{AB^{-1}}$. We have

$$\begin{aligned} B &: p_{AB} \longrightarrow p_{BA}, \\ A &: p_{BA} \longrightarrow p_{AB}, \\ B^2 &: p_{AB^2} \longrightarrow p_{B^2A}, \\ A &: p_{B^2A} \longrightarrow p_{AB^2}, \\ B^{-1} &: p_{AB^{-1}} \longrightarrow p_{B^{-1}A}, \\ A &: p_{B^{-1}A} \longrightarrow p_{AB^{-1}}. \end{aligned}$$

Up to powers of A, the cycles for the parabolic fixed points are the following

$$\begin{aligned} &p_{AB} \xrightarrow{B} p_{BA} \xrightarrow{A} p_{AB}, \\ &p_{AB^2} \xrightarrow{B^2} p_{B^2A} \xrightarrow{A} p_{AB^2}, \\ &p_{AB^{-1}} \xrightarrow{B^{-1}} p_{BA^{-1}} \xrightarrow{A} p_{AB^{-1}}. \end{aligned}$$

That is, p_{AB}, p_{AB^2} and $p_{AB^{-1}}$ are fixed by AB, AB^2 and AB^{-1} respectively. The elements AB, AB^2 and AB^{-1} are unipotent and preserve all horoballs at p_{AB}, p_{AB^2} and $p_{AB^{-1}}$ respectively.

This completes the proof of Theorem 3·6.

4. *Topology of the ideal boundary of the Ford domain D_Σ*

In this section, we study the topology at infinity of the Ford domain D_Σ of $\Sigma < \Delta_{4,\infty,\infty;\infty}$. Take the singular surface

$$\mathcal{S} = \bigcup_{k\in\mathbb{Z}} \left(\left(s_k^+ \cup s_k^- \cup s_k^\star \right) \cap \partial \mathbf{H}^2_{\mathbb{C}} \right)$$

in the Heisenberg group. Part of $\mathcal{S}$ is shown in Figures 2 and 3. The ideal boundary of a Ford domain is the intersection of the exteriors of all spinal spheres. Thus, the ideal boundary of D_Σ,

$$\partial_\infty D_\Sigma = D_\Sigma \cap \partial \mathbf{H}^2_{\mathbb{C}},$$

is the region outside $\mathcal{S}$ in Figures 2 and 3. We will show that $\partial_\infty D_\Sigma$ is an A-invariant infinite genus handlebody.

Figure 2 indicates that there are "holes" in $\partial_\infty D_\Sigma$. One "hole" with a purple boundary (the topological quadrilateral $[x_1, y_1, x_2, AB^2\ (y_1)]$) shown in Figure 3 is enclosed by the spinal spheres of I_0^+, $I_0^\star$, I_1^- and $I_1^\star$, labelled as B, B^2, $AB^{-1}A^{-1}$ and AB^2A^{-1} respectively. The "holes" make the topology of $\partial_\infty D_\Sigma$ dramatically different from that studied in [**5, 12, 13, 20**]. The ideal boundaries of the Ford domains in this literature are all infinite cylinders. Since the topology of $\partial_\infty D_\Sigma$ is complicated, we need explicit disks to cut out a 3-ball from it in our proof of Theorem 1·2.

4·1. *Two disks E_B and $E_{B^{-1}}$*

We will construct a set of disks

$$\left\{ A^k (E_B \cup E_{B^{-1}}) \right\}_{k\in\mathbb{Z}},$$

https://doi.org/10.1017/S0305004126102163 Published online by Cambridge University Press

which cap off all the "holes" in $\partial_\infty D_\Sigma$. By cutting $\partial_\infty D_\Sigma$ along these disks, we obtain an infinite cylinder, which is topologically a solid torus.

Recall the points x_i for $i = 1, 2, 3, 4$ in Section 3, and consider two additional points

$$y_1 = \begin{bmatrix} -\frac{1}{2} \\ -\frac{\sqrt{3}-i}{2} \\ 1 \end{bmatrix} \in \partial_\infty I_0^+ \cap \partial_\infty I_0^\star, \qquad y_2 = \begin{bmatrix} -\frac{1}{2} \\ -\frac{\sqrt{3}+i}{2} \\ 1 \end{bmatrix} \in \partial_\infty I_0^- \cap \partial_\infty I_0^\star.$$

Now, consider the topological circle C_B consisting of the following four arcs:

(i) let C_5 be the arc in $s_0^+ \cap \partial \mathbf{H}^2_{\mathbb{C}}$ joining x_1 to y_1 given by

$$C_5 = \left\{ \begin{bmatrix} -\frac{1}{2} - e^{2si} - i\sqrt{2\cos(2s)}e^{\frac{2s-\pi}{4}i} \\ -\sqrt{2\cos(2s)}e^{\frac{2s-\pi}{4}i} + i \\ 1 \end{bmatrix} : s \in \left[\frac{5\pi}{6}, \pi\right] \right\};$$

(ii) let C_1 be the $\mathbb{C}$-arc in $s_0^\star \cap \partial \mathbf{H}^2_{\mathbb{C}}$ joining y_1 to x_2 given by

$$C_1 = \left\{ \begin{bmatrix} -\frac{1}{2} \\ e^{is} \\ 1 \end{bmatrix} : s \in \left[\frac{5\pi}{6}, \pi\right] \right\};$$

(iii) let C_6 be the arc in $s_1^- \cap \partial \mathbf{H}^2_{\mathbb{C}}$ joining $AB^2(y_1)$ and x_1 given by

$$C_6 = \left\{ \begin{bmatrix} -\frac{5}{2} - 2i - e^{2si} + (2-i)\sqrt{2\cos(2s)}e^{\frac{2s-\pi}{4}i} \\ -2 - i + \sqrt{2\cos(2s)}e^{\frac{2s-\pi}{4}i} \\ 1 \end{bmatrix} : s \in \left[\frac{5\pi}{6}, \pi\right] \right\};$$

(iv) let C_2 be the $\mathbb{C}$-arc in $s_1^\star \cap \partial \mathbf{H}^2_{\mathbb{C}}$ joining x_2 and $AB^2(y_1)$ given by

$$C_2 = \left\{ \begin{bmatrix} -\frac{5}{2} - 2e^{is} \\ -2 - e^{is} \\ 1 \end{bmatrix} : s \in \left[\frac{5\pi}{6}, \pi\right] \right\}.$$

We will show later that the union of C_5, C_1, C_6, and C_2 forms a simple closed curve, denoted C_B. We use ruled surfaces to construct a disk E_B with boundary C_B. One ruled surface, with directrices C_5 and C_1, is denoted by E_B^l; another, with directrices C_6 and C_2, is denoted by E_B^r. Let c_i represents the coordinates of C_i in $\mathcal{N}$ for $i = 1, 2, 5, 6$. The ruled surfaces can be described as

$$E_B^l = (1-a)\cdot c_5 + a \cdot c_1, \quad E_B^r = (1-a)\cdot c_6 + a \cdot c_2$$

for $a \in [0, 1]$. In Figure 5, E_B^l is shown in blue and E_B^r in green. We define $E_B = E_B^l \cup E_B^r$. It is easy to verify that $E_B^l \cap E_B^r$ is the straight-line segment from x_1 to x_2 in $\mathcal{N}$. In Figure 5, E_B patches up the "hole" of $\partial_\infty D_\Sigma$ enclosed by the spinal spheres $\partial_\infty I_0^+$, $\partial_\infty I_1^-$, $\partial_\infty I_0^\star$ and $\partial_\infty I_1^\star$.

https://doi.org/10.1017/S0305004126102163 Published online by Cambridge University Press

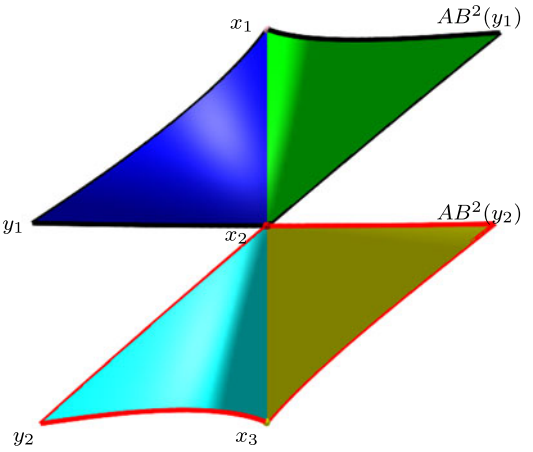


Figure 5. The disks EB (the union of the blue triangle $[x_1, y_1, x_2]$ and green triangle $[x_1, x_2, AB^2(y_1)]$) and EB-1 (the union of the cyan triangle $[x_2, y_2, x_3]$ and yellow triangle $[x_2, x_3, AB^2(y_2)]$).

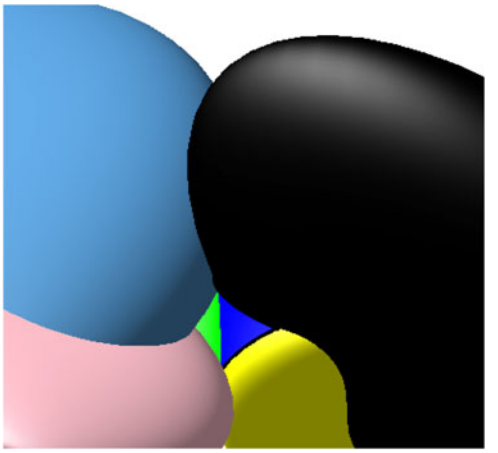


Figure 6. The disk E_B caps off the "hole" of $\partial_\infty D_\Sigma$ enclosed by the spinal spheres $\partial_\infty I_0^+$ (black, remaining black in print), $\partial_\infty I_1^-$ (steelblue, appearing grey in print), $\partial_\infty I_0^\star$ (yellow, appearing light grey in print) and $\partial_\infty I_1^\star$ (pink, appearing light grey in print).

As an example, we give the Heisenberg coordinates of E_B^l:

$$\begin{cases} x = \cos(s)a - \sqrt{2\cos(2s)}\sin\frac{2s+\pi}{4}\cdot(1-a) \\ y = \sin(s)a + \left(1+\sqrt{2\cos(2s)}\cos\frac{2s+\pi}{4}\right)\cdot(1-a) \\ t = -2\left(\sin(2s) + \sqrt{2\cos(2s)}\sin\frac{2s+\pi}{4}\right)\cdot(1-a), \end{cases} \tag{4·1}$$

where $a \in [0, 1]$ and $s \in [5\pi/6, \pi]$. We use projection mapping to give results on whether E_B^l intersects the spinal spheres.

LEMMA 4·1. *Let $\Pi : \mathcal{N} \longrightarrow \mathbb{C}$ be the nature projection. The union of $\Pi(C_5)$ and $\Pi(C_1)$ is a simple closed curve in $\mathbb{C}$ contained in $\Pi(\partial_\infty I_0^-)$ and $\Pi(\partial_\infty I_1^-)$. Besides,*

https://doi.org/10.1017/S0305004126102163 Published online by Cambridge University Press

(i) $\Pi(E_B^l)$ *intersects* $\Pi(\partial_\infty I_0^-)$ *and* $\Pi(\partial_\infty I_1^-)$ *at the same point* $\Pi(x_1)$*;*

(ii) $\Pi(E_B^l)$ *intersects* $\Pi(\partial_\infty I_0^*)$ *to be the arc* $\Pi(C_1)$*;*

(iii) $\Pi(E_B^l)$ *intersects* $\Pi(\partial_\infty I_k^* \cup \partial_\infty I_k^+ \cup \partial_\infty I_k^-)_{k\in\mathbb{Z}}$ *to be the empty set for* $k \neq 0, 1$.

Proof. According to the equations of C_5 and C_1, it is easy to know

$$\Pi(C_5) \cap \Pi(C_1) = \Pi(y_1) \cup \Pi(x_1).$$

So $\Pi(C_5) \cup \Pi(C_1)$ is a simple closed curve. It is also easy to check that $\Pi(C_5)$ and $\Pi(C_1)$ are all contained in $\Pi(\partial_\infty I_1^+)$ and $\Pi(\partial_\infty I_0^+)$. We have completed the first half of the proof.

For (i), according to

$$\Pi(x_1) = \Pi(x_2) = \Pi(\partial_\infty I_0^+) \cap \Pi(\partial_\infty I_1^-) = \Pi\big(\partial_\infty I_0^-\big) \cap \Pi(\partial_\infty I_1^+),$$

and the affine convexity of $\Pi(\partial_\infty I_0^+)$ and $\Pi(\partial_\infty I_1^+)$, we know that

$$\Pi\big(E_B^l\big) \cap \Pi\big(\partial_\infty I_0^-\big) = \Pi\big(E_B^l\big) \cap \Pi\big(\partial_\infty I_1^-\big) = \Pi(x_1).$$

For (ii), we prove that for a given $s \in [5\pi/6, \pi]$, the projection of each straight line on E_B^l, with parameterisation (4.1), intersects $\Pi(C_1)$ at one point. Write $d_u = \big(\cos(s), \sin(s)\big)$, which is the coordinate of some point in $\Pi(C_1)$. It is also the vector from the origin O in $\mathbb{C}$ to this point. Write $d_l = \big(\partial x/\partial a, \partial y/\partial a\big)\big|_{a=1}$, which is the direction of the projection of the straight line on E_B^l. Note that when $a = 0$, the corresponding point of E_B^l is in C_5, and when $a = 1$, the corresponding point is in C_1. By calculating the inner product of $-d_l$ and d_u, we can determine whether the point in the straight line of $\Pi(E_B^l)$ is far away from $\Pi(C_1)$ when a decreases from 1 to 0. In fact, the inner product of $-d_l$ and d_u is

$$\begin{aligned}&\left(\sin\left(\frac{s}{2}\right) - \cos\left(\frac{s}{2}\right)\right)\sqrt{\cos(2s)} + \sin(s) - 1\\ &= -\sqrt{2}\sin\left(\frac{\pi}{4} - \frac{s}{2}\right)\cdot\left(\sqrt{2}\sin\left(\frac{\pi}{4} - \frac{s}{2}\right) + \sqrt{\cos(2s)}\right),\end{aligned}$$

which is non-negative when $s \in [5\pi/6, \pi]$. By the affine convexity of $\Pi(\partial_\infty I_0^\star)$, we have $\Pi(E_B^l) \cap \Pi(\partial_\infty I_0^\star) = \Pi(C_1)$.

For (iii), because

$$\Pi\big(E_B^l\big) \subset \Pi\big(\partial_\infty I_0^-\big) \cap \Pi\big(\partial_\infty I_1^-\big),$$

which is outside all $\Pi(\partial_\infty I_k^* \cup \partial_\infty I_k^+ \cup \partial_\infty I_k^-)_{k\in\mathbb{Z}}$ for $k \neq 0, 1$, we get the conclusion.

Instead of depicting the entire projections of E_B^l and E_B^r, we show the projections of several representative straight lines from these surfaces in Figure 7, represented by blue and green segments, respectively. The projections of E_B and $E_{B^{-1}}$ are the union of blue and green crescents and the union of yellow and cyan crescents respectively. The projection of $\partial_\infty I_0^+$, $\partial_\infty I_0^-$, $\partial_\infty I_1^+$ and $\partial_\infty I_1^-$ are the round disk with radius $\sqrt{2}$ and centered at i, $-i$, $-2+i$ and $-2-i$, respectively. The projections of $\partial_\infty I_0^\star$ and $\partial_\infty I_1^\star$ are round disks with radius 1 and centered at 0 and -2 respectively. The projection of F is the union of magenta, coral and navy curves. (Colours online. In print: blue and navy appear as dark grey; green, yellow, cyan and coral appear as light grey; magenta appears as grey.) Figure 8 gives an enlarged view of $\Pi(E_B^l)$.

https://doi.org/10.1017/S0305004126102163 Published online by Cambridge University Press

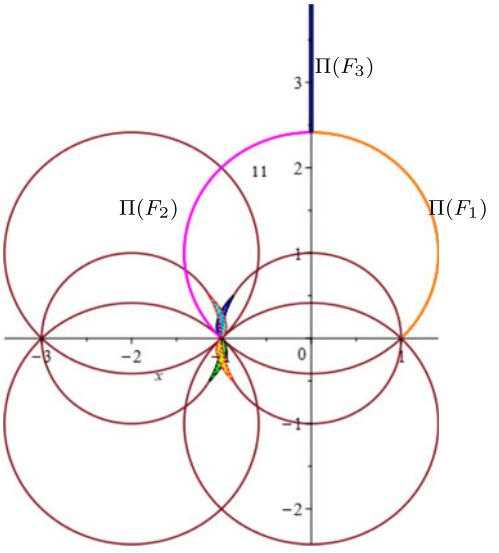


Figure 7. The projections of $\partial_\infty I_0^{\pm}$, $\partial_\infty I_1^{\pm}$, $\partial_\infty I_0^{\star}$, $\partial_\infty I_1^{\star}$, E_B, $E_{B^{-1}}$ and F.

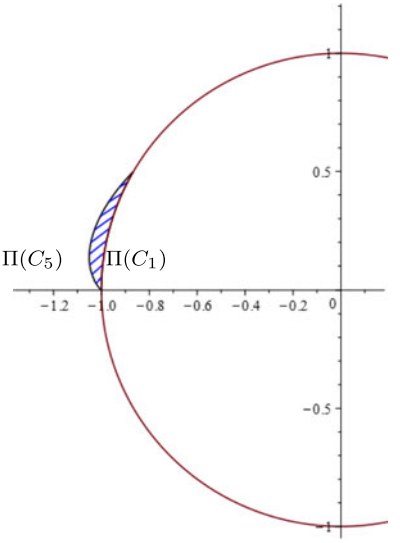


Figure 8. An enlarged view of $\Pi(E_B^l)$ and part of $\Pi(\partial_\infty I_0^{\star})$.

For the relationship between E_B^l and the remaining spinal spheres, we have:

LEMMA 4·2. *For* $E_B^l \cap (\partial_\infty I_0^+ \cup \partial_\infty I_1^+ \cup \partial_\infty I_0^*)$, *we have*:

(i) $E_B^l \cap \partial_\infty I_0^+ = C_5$;
(ii) $E_B^l \cap \partial_\infty I_1^* = x_2$;
(iii) $E_B^l \cap \partial_\infty I_1^+ = \emptyset$.

https://doi.org/10.1017/S0305004126102163 Published online by Cambridge University Press

Proof. Let $p(s,a)=(x(s,a),y(s,a),t(s,a))\in E_B^l$ be the point given by Equation (4.1). For (i), consider the Cygan distance between $B^{-1}(q_\infty)$ and $p(s,a)$. Let

$$g(s,a)=d_{\mathrm{Cyg}}^4\big(B^{-1}(q_\infty),p\big)=\big(x^2+(y-1)^2\big)^2+(t-2x)^2$$

with $a\in[0,1]$ and $s\in[5\pi/6,\pi]$. Then

$$\begin{aligned}\frac{\partial g(s,a)}{\partial a}\Big|_{a=0}&=16\cos^{3/2}(2s)\left(\sin\frac{s}{2}-\cos\frac{s}{2}\right)+4(\sin(3s)-\cos(4s)+\sin(s))-12\\&\geq 0,\end{aligned}$$

for $s\in[5\pi/6,\pi]$ by Lemma 4·3 later. By the affine convexity of the isometric spheres, we know that for $a\in[0,1]$ and $s\in[5\pi/6,\pi]$,

$$d_{\mathrm{Cyg}}\big(B^{-1}(q_\infty),p(s,a)\big)\geq d_{\mathrm{Cyg}}\big(B^{-1}(q_\infty),p(s,0)\big),$$

and the equality holds if and only if $a=0$, which are points on C_5.

For (ii), let

$$h(s,a)=d_{\mathrm{Cyg}}^4\big(AB^2A^{-1}(q_\infty),p(s,a)\big)=((x+2)^2+y^2)^2+(t-2y)^2,$$

where $a\in[0,1]$ and $s\in[5\pi/6,\pi]$. By Lemma 4·3 later, we have

$$\begin{aligned}\frac{\partial h(s,a)}{\partial a}\Big|_{a=1}&=\left(96\cos^3\frac{s}{2}+12\cos\frac{s}{2}+4\sin\frac{s}{2}\right)\sqrt{\cos(2s)}+52\cos(s)-28\sin(s)\\&\quad+12\cos(2s)+4\cos(3s)-8\sin(2s)+40\leq 0,\end{aligned}$$

for $s\in[5\pi/6,\pi]$. By the affine convexity of the isometric spheres, we know that for $a\in[0,1]$ and $s\in[5\pi/6,\pi]$,

$$d_{\mathrm{Cyg}}\big(AB^2A^{-1}(q_\infty),p(s,a)\big)\geq d_{\mathrm{Cyg}}\big(AB^2A^{-1}(q_\infty),p(s,1)\big)\geq 1.$$

The first equality holds if and only if $a=1$, and the second equality holds if and only if $s=\pi$, corresponding to the point x_2.

For (iii), consider the plane

$$-3(X+1+Y)+T=0$$

in the Heisenberg group. On the one hand, it is easy to check that $t-3(x+1+y)\leq 0$, and the equality holds if and only if $p(s,a)=x_2$. On the other hand,

$$\partial_\infty I_1^+=\left\{\begin{bmatrix}2i-e^{-\alpha i}\pm(2+i)\sqrt{2\cos\alpha}\cdot e^{(-\frac{\alpha}{2}+\beta)i}-\frac{5}{2}\\-2+i\pm\sqrt{2\cos\alpha}\cdot e^{(-\frac{\alpha}{2}+\beta)i}\\1\end{bmatrix}:\alpha\in\left[-\frac{\pi}{2},\frac{\pi}{2}\right],\ \beta\in[0,\pi)\right\}.$$

Let $p_0\in\partial_\infty I_1^+$ be a point with Heisenberg coordinates (x_0,y_0,t_0). Then

$$\begin{aligned}-3(x_0+1+y_0)+t_0&=\mp\sqrt{2\cos\alpha}\left(\cos\left(\frac{\alpha}{2}-\beta\right)+\sin\left(\frac{\alpha}{2}-\beta\right)\right)+2\sin\alpha+4\\&\geq-2\sqrt{\cos\alpha}+2\sin\alpha+4>0.\end{aligned}$$

Hence, E_B^l and $\partial_\infty I_1^+$ are separated by the above plane.

https://doi.org/10.1017/S0305004126102163 Published online by Cambridge University Press

LEMMA 4·3. *Let*

$$f_1(s) = 16\cos^{3/2}(2s)\left(\sin\frac{s}{2} - \cos\frac{s}{2}\right) + 4(\sin(3s) - \cos(4s) + \sin(s)) - 12$$

and

$$f_2(s) = \left(96\cos^3\frac{s}{2} + 12\cos\frac{s}{2} + 4\sin\frac{s}{2}\right)\sqrt{\cos(2s)} + 52\cos(s) - 28\sin(s) + 12\cos(2s) + 4\cos(3s) - 8\sin(2s) + 40$$

be two functions. For $s \in [5\pi/6, \pi]$, *we have*:

(i) $f_1(s) \geq 0$, *and the equality holds if and only if* $s = 5\pi/6$ *or* $s = \pi$;

(ii) $f_2(s) \leq 0$, *and the equality holds if and only if* $s = 5\pi/6$ *or* $s = \pi$.

Proof. For (i), it is easy to see that $4\cos^{3/2}(2s)(\sin\frac{s}{2} - \cos\frac{s}{2}) > 0$ and

$$-\sin(3s) + \cos(4s) - \sin(s) + 3 > 0$$

when $s \in [5\pi/6, \pi]$. Then

$$\frac{f_1(s)}{2} \cdot \left(4\cos^{3/2}(2s)\left(\sin\frac{s}{2} - \cos\frac{s}{2}\right) + (-\sin(3s) + \cos(4s) - \sin(s) + 3)\right)$$
$$= -21 + 9\cos(6s) - 10\cos(4s) + 6\sin(5s) - 2\sin(3s) + 22\sin(s) + 23\cos(2s) - \cos(8s) - 2\sin(7s).$$

Let $x = \sin(s)$, the above equation is written as:

$$F_1(x) = -32x(2x-1)(2x^6 - x^5 + 2x^3 - 2x^2 - x + 1),$$

where $x \in [0, 1/2]$. Observe that $2x^6 - x^5 + 2x^3 = x^3(2x^3 + 2 - x^2) > 0$ and $1 - 2x^2 - x > 0$ for $x \in (0, 1/2)$. The roots of $F_1(x)$ in $[0, 1/2]$ are only 0 and $1/2$. Thus we have that $f_1(s) \geq 0$, and the equality holds exactly when $s = 5\pi/6$ or $s = \pi$.

For (ii), it is easy to see that

$$\left(24\cos^3\frac{s}{2} + 3\cos\frac{s}{2} + \sin\frac{s}{2}\right)\sqrt{\cos(2s)} > 0$$

and

$$13\cos(s) - 7\sin(s) + 4\cos(2s) + \cos(3s) - 2\sin(2s) + 10 < 0$$

when $s \in [5\pi/6, \pi]$. Then

$$\frac{f_2(s)}{2} \cdot \left(\left(24\cos^3\frac{s}{2} + 3\cos\frac{s}{2} + \sin\frac{s}{2}\right)\sqrt{\cos(2s)} - \left(13\cos(s) - 7\sin(s) + 4\cos(2s) + \cos(3s) - 2\sin(2s) + 10\right)\right)$$
$$= -306 + 32\sin(4s) - \cos(6s) + 248\sin(2s) + 95\cos(4s) + 4\sin(5s) + 109\sin(3s) - 268\cos(s) + 271\sin(s) + 212\cos(2s) + 256\cos(3s) + 12\cos(5s).$$

Let $x = \sin(s)$, the above equation is written as:

$$F_2(x) = 32\left(x - \frac{1}{2}\right)x\left((39 - 6x^2 + 5x)\sqrt{1-x^2} + x^4 + \frac{5x^3}{2} + \frac{47x^2}{2} - \frac{35x}{8} - \frac{309}{8}\right),$$

https://doi.org/10.1017/S0305004126102163 Published online by Cambridge University Press

where $x \in [0, 1/2]$. Define

$$G(x) = (39 - 6x^2 + 5x)\sqrt{1-x^2} + x^4 + \frac{5x^3}{2} + \frac{47x^2}{2} - \frac{35x}{8} - \frac{309}{8}.$$

We claim that $G(x) > 0$ for $x \in [0, 1/2]$. Note that $\sqrt{1-x^2} \geq 1 - x^2/2 - x^4/6$ and $39 - 6x^2 + 5x > 0$ for $x \in [0, 1/2]$. Then

$$\begin{aligned} G(x) &\geq (39 - 6x^2 + 5x)\left(1 - \frac{x^2}{2} - \frac{x^4}{6}\right) + x^4 + \frac{5x^3}{2} + \frac{47x^2}{2} - \frac{35x}{8} - \frac{309}{8} \\ &= x^6 - \frac{5}{6}x^5 - \frac{5}{2}x^4 - 2x^2 + \frac{5}{8}x + \frac{3}{8} \\ &= \left(x - \frac{1}{2}\right)^6 + \frac{13}{6}x\left(x - \frac{1}{2}\right)^4 - \frac{23}{12}x^4 - \frac{3}{4}x^3 - \frac{89}{48}x^2 + \frac{65}{96}x + \frac{23}{64}. \end{aligned}$$

It is easy to verify that $45/96x - 23/12x^4 - 3/4x^3 \geq 0$ and $-89/48x^2 + 20/96x + 23/64 \geq 0$ for $x \in [0, 1/2]$. Then we have $-23/12x^4 - 3/4x^3 - 89/48x^2 + 65/96x + 23/64 \geq 0$ for $x \in [0, 1/2]$. Now we have that $F_2(x) \leq 0$ and the roots of $F_2(x)$ in $[0, 1/2]$ are only 0 and $1/2$. Hence $f_2(s) \leq 0$, and the equality holds exactly when $s = 5\pi/6$ or $s = \pi$.

Now, we have completed the proofs of (ii) and (iii) of Proposition 4·4 below.

PROPOSITION 4·4. *We have*:

(i) *the union of C_5, C_1, C_6 and C_2 is a simple closed curve C_B;*

(ii) *C_B bounds the disk E_B. The interior of E_B is disjoint from $\partial_\infty I_k^* \cup \partial_\infty I_k^+ \cup \partial_\infty I_k^-$ for any $k \in \mathbb{Z}$;*

(iii) *$E_B \cap A^k(E_B) = \emptyset$ if $k \neq 0$.*

Proof. For (i), by Proposition 3·4, we know that $I_0^\star \cap I_1^- = \emptyset$, $I_0^\star \cap I_1^\star = x_2$, $I_0^+ \cap I_1^- = x_1$, and $I_0^+ \cap I_1^\star = \emptyset$. The curves C_5, C_1, C_6 and C_2 are contained in I_0^+, $I_0^\star$, $I_1^\star$ and I_1^-, respectively. Therefore, we need only to check that $C_5 \cap C_1 = y_1$. By the equations of C_5 and C_1, we have $C_5 \cap C_1$ is given by

$$\begin{bmatrix} -\frac{1}{2} - e^{2si} - i\sqrt{2\cos(2s)}e^{\frac{2s-\pi}{4}i} \\ -\sqrt{2\cos(2s)}e^{\frac{2s-\pi}{4}i} + i \\ 1 \end{bmatrix} = \begin{bmatrix} -\frac{1}{2} \\ e^{s'} \\ 1 \end{bmatrix}$$

for some $s, s' \in [5\pi/6, \pi]$. This holds if and only if $s = s' = 5\pi/6$, which corresponds to the point y_1.

Another topological circle $C_{B^{-1}}$ consisting of four arcs:

(i) let C_7 be the arc in $s_0^- \cap \partial\mathbf{H}^2_{\mathbb{C}}$ joining y_2 and x_3 given by

$$C_7 = \left\{ \begin{bmatrix} -\frac{1}{2} - e^{2si} + \sqrt{2\cos(2s)}e^{\frac{\pi+2s}{4}i} \\ -i + i\sqrt{2\cos(2s)}e^{\frac{\pi+2s}{4}i} \\ 1 \end{bmatrix} : s \in \left[0, \frac{\pi}{6}\right] \right\};$$

https://doi.org/10.1017/S0305004126102163 Published online by Cambridge University Press

(ii) let C_3 be the $\mathbb{C}$-arc in $s_0^\star \cap \partial\mathbf{H}^2_{\mathbb{C}}$ joining x_2 and y_2 given by

$$C_3 = \left\{ \begin{bmatrix} -\frac{1}{2} \\ -e^{si} \\ 1 \end{bmatrix} : s \in \left[0, \frac{\pi}{6}\right] \right\};$$

(iii) let C_8 be the arc in $s_1^+ \cap \partial\mathbf{H}^2_{\mathbb{C}}$ joining x_3 and $AB^2(y_2)$ given by

$$C_8 = \left\{ \begin{bmatrix} -\frac{5}{2} + 2i - e^{2si} + (1-2i)\sqrt{2\cos(2s)}e^{\frac{\pi+2s}{4}i} \\ -2 + i - i\sqrt{2\cos(2s)}e^{\frac{\pi+2s}{4}i} \\ 1 \end{bmatrix} : s \in \left[0, \frac{\pi}{6}\right] \right\};$$

(iv) let C_4 be the $\mathbb{C}$-arc in $s_1^\star \cap \partial\mathbf{H}^2_{\mathbb{C}}$ joining $AB^2(y_2)$ and x_2 given by

$$C_4 = \left\{ \begin{bmatrix} -\frac{5}{2} + 2e^{si} \\ -2 + e^{si} \\ 1 \end{bmatrix} : s \in \left[0, \frac{\pi}{6}\right] \right\}.$$

Similarly, let c_i represent the coordinates of C_i in $\mathcal{N}$ for $i = 3, 4, 7, 8$. We then construct two more ruled surfaces:

$$E^l_{B^{-1}} = (1-a)\cdot c_8 + a \cdot c_4, \quad E^r_{B^{-1}} = (1-a)\cdot c_7 + a \cdot c_3$$

with $a \in [0, 1]$.

Define $E_{B^{-1}} = E^l_{B^{-1}} \cup E^r_{B^{-1}}$. We also have $E^l_{B^{-1}} \cap E^r_{B^{-1}}$ is the straight-line segment from x_3 to x_2 in $\mathcal{N}$. In Figure 5, $E^l_{B^{-1}}$ is the cyan part, and $E^r_{B^{-1}}$ is the yellow part. The proof of Proposition 4·5 is similar to the proof of Proposition 4·4, and we omit it.

PROPOSITION 4·5. *We have*:

(i) *the union of C_7, C_3, C_8 and C_4 is a simple closed curve $C_{B^{-1}}$;*

(ii) *$C_{B^{-1}}$ bounds the disk $E_{B^{-1}} \subset \partial\mathbf{H}^2_{\mathbb{C}}$. The interior of $E_{B^{-1}}$ is disjoint from $\partial_\infty I_k^+ \cup \partial_\infty I_k^- \cup \partial_\infty I_k^*$ for any $k \in \mathbb{Z}$;*

(iii) *$E_{B^{-1}} \cap A^k(E_{B^{-1}}) = \emptyset$ if $k \neq 0$.*

From the equations of E_B and $E_{B^{-1}}$, we have:

PROPOSITION 4·6. *The disk E_B intersects the disk $E_{B^{-1}}$ exactly at the point x_2.*

PROPOSITION 4·7. *There is an unknotted infinite line $\mathcal{L}$ in $\partial\mathbf{H}^2_{\mathbb{C}}$ such that*:

(i) *$\mathcal{L} \cap \left(\mathcal{S} \cup_{k\in\mathbb{Z}} A^k(E_B \cup E_{B^{-1}})\right)$ is exactly the set $\cup_{k\in\mathbb{Z}} A^k(x_2)$;*

(ii) *the complement of $\mathcal{S} \cup_{k\in\mathbb{Z}} A^k(E_B \cup E_{B^{-1}})$ in $\partial\mathbf{H}^2_{\mathbb{C}}$ is an A-invariant $(\mathbb{R}^2 - \mathbb{D}^2) \times \mathbb{R}$ topologically.*

Proof. Let $\mathcal{L}$ be the line

$$\{[x, 0] : x \in \mathbb{R}\}$$

in $\mathcal{N}$. Then item (i) can be checked directly.

https://doi.org/10.1017/S0305004126102163 Published online by Cambridge University Press

Now, the complement of $\mathcal{S} \cup_{k\in\mathbb{Z}} A^k(E_B \cup E_{B^{-1}})$ in $\partial\mathbf{H}^2_{\mathbb{C}}$ is isotopic to the boundary of a small neighborhood of $\mathcal{L} \cup_{k\in\mathbb{Z}} A^k(E_B \cup E_{B^{-1}})$. Moreover, this isotopy can be performed in an A-equivariant fashion. Therefore, the complement is topologically an A-invariant $(\mathbb{R}^2 - \mathbb{D}^2) \times \mathbb{R}$.

4·2. *Three more disks and seventeen more arcs*

More disks are used to cut out a 3-ball in $\partial_\infty D_\Sigma$. The quotient space of this 3-ball by suitable side-parings is the 3-manifold at infinity in Theorem 1·2.

(i) let C_{17} be the $\mathbb{C}$-arc in $s_0^+ \cap \partial\mathbf{H}^2_{\mathbb{C}}$ joining x_1 and $B^{-1}(x_3)$ given by

$$C_{17} = \left\{ \begin{bmatrix} -\frac{3}{2} - i\sqrt{2}e^{is} \\ i - \sqrt{2}e^{is} \\ 1 \end{bmatrix} : s \in \left[\frac{3\pi}{4}, \frac{9\pi}{4}\right] \right\}.$$

(ii) let C_{19} be the $\mathbb{C}$-arc in $\partial\mathbf{H}^2_{\mathbb{C}}$ joining q_∞ and $B^{-1}(x_3)$ given by

$$C_{19} = \left\{ \begin{bmatrix} -\frac{1}{2} + si \\ 1 \\ 1 \end{bmatrix} : s \in [2, \infty] \right\}.$$

(iii) let C_{20} be the $\mathbb{C}$-arc in $\partial\mathbf{H}^2_{\mathbb{C}}$ joining x_1 and q_∞ given by

$$C_{20} = \left\{ \begin{bmatrix} -\frac{1}{2} - si \\ -1 \\ 1 \end{bmatrix} : s \in [2, \infty] \right\}.$$

Now, we construct a disk F. First, we take vertical upward rays (part of $\mathbb{C}$-arcs) along the first half of C_{17}, with paramatrization

$$[-\sqrt{2}\cos(s), 1 - \sqrt{2}\sin(s), -2\sqrt{2}\cos(s) + a]$$

in Heisenberg coordinates with $s \in [3\pi/4, 3\pi/2]$ and $a \in [0, +\infty]$. Denote this part by F_1. Next, we take vertical downward rays (part of the $\mathbb{C}$-arcs) along the second half of C_{17}, with paramatrization

$$[-\sqrt{2}\cos(s), 1 - \sqrt{2}\sin(s), -2\sqrt{2}\cos(s) + a]$$

in Heisenberg coordinates with $s \in [3\pi/2, 9\pi/4]$ and $a \in [0, -\infty]$. Denote this part by F_2. Finally, we take a vertical half-plane F_3, with paramatrization

$$[0, (1 + \sqrt{2})s, t]$$

in Heisenberg coordinates with $s \in [1 + \infty]$ and $t \in [-\infty, +\infty]$. Let

$$C_F = C_{17} \cup C_{19} \cup C_{20} \quad \text{and} \quad F = F_1 \cup F_2 \cup F_3.$$

They are shown in Figure 10. We draw a part of F together with several spinal spheres in Figure 11. Using the previous method similarly, we give the following results.

https://doi.org/10.1017/S0305004126102163 Published online by Cambridge University Press

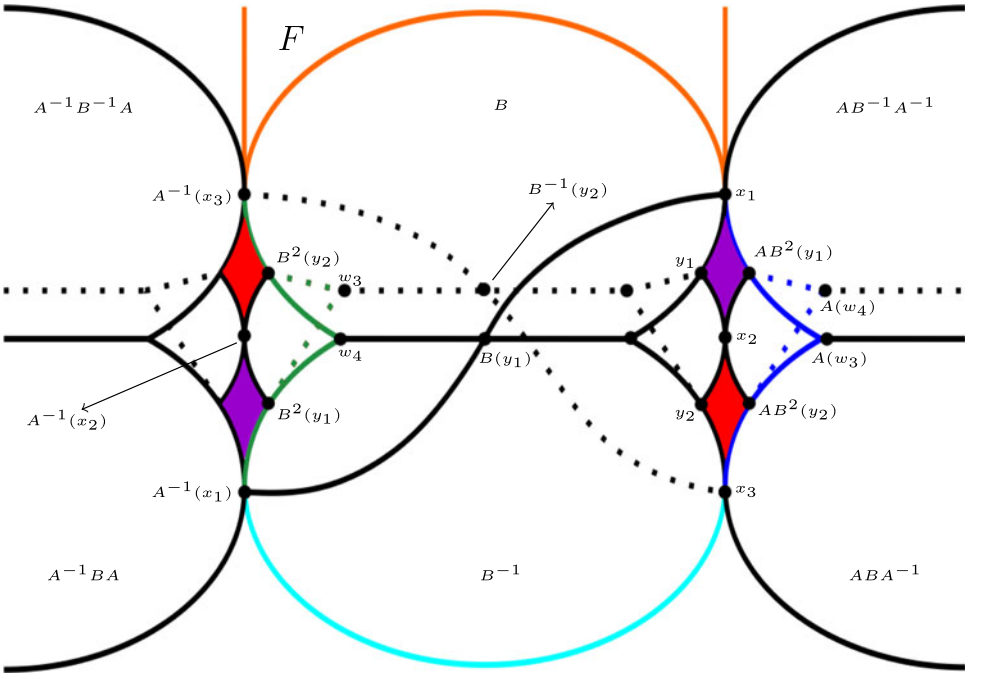


Figure 9. The topology of the Ford domain of $\Delta_{4,\infty,\infty;\infty}$. After capping off the holes in Figure 2 by red disks (the quadrilaterals $[A^{-1}(x_3), A^{-1}(y_2), A^{-1}(x_2), B^2(y_2)]$ and $[x_2, y_2, x_3, AB^2(y_2)]$) and purple disks (the quadrilaterals $[A^{-1}(x_2), A^{-1}(y_1), A^{-1}(x_1), B^2(y_1)]$ and $[x_1, y_1, x_2, AB^2(y_1)]$), we need two once-punctured disks D_- and D_+, and a triangle F. The boundary of D_- (green) is the curve $[A^{-1}(x_3), B^2(y_2), w_4, B^2(y_1), A^{-1}(x_1), B^2(y_1), w_3, B^2(y_2), A^{-1}(x_3)]$, the boundary of D_+ (blue) is the curve $[x_1, AB^2(y_1), A(w_3), AB^2(y_2), x_3, AB^2(y_2), A(w_4), AB^2(y_1), x_1]$, and the triangle F has an orange boundary (online; light grey in print).

PROPOSITION 4·8. *We have*:

(i) *the union C_F is a simple closed curve;*

(ii) *C_F bounds the disk $F \subset \partial\mathbf{H}^2_{\mathbb{C}}$. The interior of F has no intersection with $\partial_\infty I_k^+ \cup \partial_\infty I_k^- \cup \partial_\infty I_k^*$ for any $k \in \mathbb{Z}$.*

Proof. For item (i), by the equations of the arcs of C_F, it is easy to verify that any pair intersect only at one end point.

For item (ii), according to the structure of F, we naturally have $\partial F = C_F$. First, the projection $\Pi(F_3)$ is a ray in $\mathbb{C}$, satisfying

$$\Pi\big(F_3 \cap (\partial_\infty I_k^+ \cup \partial_\infty I_k^- \cup \partial_\infty I_k^*)\big) = (0, 1+\sqrt{2}) \in \Pi(\partial_\infty I_0^+).$$

Second,

$$\Pi(F_2) = \big(-\sqrt{2}\cos(s), 1-\sqrt{2}\sin(s)\big) \subset \partial\Pi(\partial_\infty I_0^+),$$

where $s \in [3\pi/4, 3\pi/2]$. Therefore, the interior of F_2 is disjoint from $\partial_\infty I_k^+ (k \neq 1)$, $\partial_\infty I_k^-$, and $\partial_\infty I_k^\star (k \neq 1)$ for $k \in \mathbb{Z}$. We need only to check that if $F_2 \cap (\partial_\infty I_1^+ \cup \partial_\infty I_1^\star)$ is an empty set.

https://doi.org/10.1017/S0305004126102163 Published online by Cambridge University Press

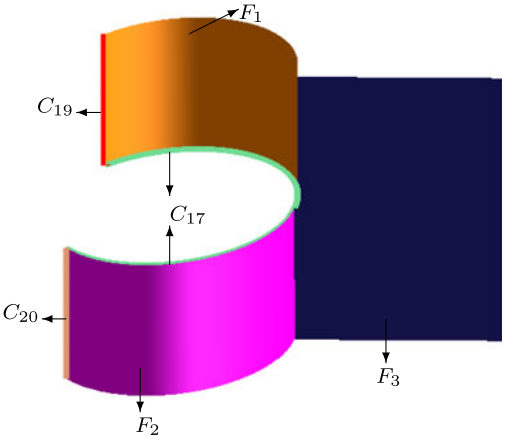


Figure 10. Disks F_1 (coral), F_2 (magenta) and F_3 (blue), curves C_{17} (green), C_{19} (red) and C_{20} (tan).

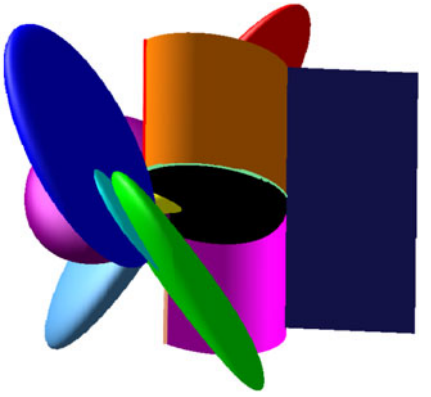


Figure 11. Add part of the disk F to Figure 2.

On the one hand, consider the plane

$$3(X+1+Y)-2-T=0$$

in the Heisenberg group. For any point $(x_0, y_0, t) \in F_2$, where $(x_0, y_0, t_0) \in C_{17}^1$ and $t \le t_0$, we have

$$\begin{aligned} 3(x_0+1+y_0)-2-t &\ge 3(x_0+1+y_0)-2-t_0 \\ &= 3(-\sqrt{2}\cos(s)+1+1-\sqrt{2}\sin(s))-2+2\sqrt{2}\cos(s) \\ &= 4-\sqrt{2}\cos(s)-3\sqrt{2}\sin(s) \ge 0. \end{aligned}$$

This means that F_2 is on one side of this plane.

On the other hand, for any point $(x_0, y_0, t_0) \in s_1^+$,

$$\begin{aligned} 3(x_0+1+y_0)-2-t_0 &= \mp\sqrt{2\cos\alpha}\left(\cos\left(\frac{\alpha}{2}-\beta\right)+\sin\left(\frac{\alpha}{2}-\beta\right)\right)-2\sin\alpha-6 \\ &\le 2\sqrt{\cos\alpha}-2\sin\alpha-6<0. \end{aligned}$$

https://doi.org/10.1017/S0305004126102163 Published online by Cambridge University Press

Table I. *Some curve information*

Name	Ends	Belongs to
$C_{18} = B(C_{17})$	$x_3, B(x_1)$	$s_0^- \cap \partial\mathbf{H}^2_{\mathbb{C}}$
$C_9 = A^{-1}(C_2)$	$A^{-1}(x_2), B^2(y_1)$	$s_0^* \cap \partial\mathbf{H}^2_{\mathbb{C}}$
$C_{10} = A^{-1}(C_4)$	$A^{-1}(x_2), B^2(y_2)$	$s_0^* \cap \partial\mathbf{H}^2_{\mathbb{C}}$
$C_{11} = A^{-1}(C_6)$	$A^{-1}(x_1), B^2(y_1)$	$s_0^- \cap \partial\mathbf{H}^2_{\mathbb{C}}$
$C_{12} = A^{-1}(C_8)$	$A^{-1}(x_3), B^2(y_2)$	$s_0^+ \cap \partial\mathbf{H}^2_{\mathbb{C}}$
$C_{13} = B(C_5)$	$B(x_1), B(y_1)$	$s_0^- \cap \partial\mathbf{H}^2_{\mathbb{C}}$
$C_{14} = B^{-1}A^{-1}(C_6)$	$x_1, B(y_1)$	$s_0^+ \cap \partial\mathbf{H}^2_{\mathbb{C}}$
$C_{15} = B^{-1}(C_7)$	$B^{-1}(x_3), B^{-1}(y_3)$	$s_0^+ \cap \partial\mathbf{H}^2_{\mathbb{C}}$
$C_{16} = BA^{-1}(C_8)$	$x_3, B(y_1)$	$s_0^- \cap \partial\mathbf{H}^2_{\mathbb{C}}$
C_{21}	$AB^2(y_1), A(w_3)$	$s_1^- \cap s_1^* \cap \partial\mathbf{H}^2_{\mathbb{C}}$
C_{22}	$AB^2(y_1), A(w_4)$	$s_0^- \cap s_1^* \cap \partial\mathbf{H}^2_{\mathbb{C}}$
C_{23}	$AB^2(y_2), A(w_3)$	$s_1^+ \cap s_1^* \cap \partial\mathbf{H}^2_{\mathbb{C}}$
C_{24}	$AB^2(y_2), A(w_4)$	$s_1^+ \cap s_1^* \cap \partial\mathbf{H}^2_{\mathbb{C}}$
$C_{25} = B^{-1}A^{-1}(C_{22})$	$w_1, B(y_1)$	$s_0^+ \cap s_0^- \cap \partial\mathbf{H}^2_{\mathbb{C}}$
$C_{26} = B^{-1}A^{-1}(C_{21})$	$w_4, B(y_1)$	$s_0^+ \cap s_0^- \cap \partial\mathbf{H}^2_{\mathbb{C}}$
$C_{27} = BA^{-1}(C_{24})$	$w_3, B^{-1}(y_3)$	$s_0^+ \cap s_0^- \cap \partial\mathbf{H}^2_{\mathbb{C}}$
$C_{28} = BA^{-1}(C_{23})$	$w_2, B^{-1}(y_3)$	$s_0^+ \cap s_0^- \cap \partial\mathbf{H}^2_{\mathbb{C}}$

Moreover,

$$\partial_\infty I_1^* = \left\{ \begin{bmatrix} -\frac{e^{-\alpha i}}{2} \pm 2\sqrt{\cos\alpha}\cdot e^{(-\frac{\alpha}{2}+\beta)i} - 2 \\ -2 \pm \sqrt{\cos\alpha}\cdot e^{(-\frac{\alpha}{2}+\beta)i} \\ 1 \end{bmatrix} : \alpha \in \left[-\frac{\pi}{2}, \frac{\pi}{2}\right],\ \beta \in [0,\pi) \right\}.$$

So for any point $(x_0, y_0, t_0) \in \partial_\infty I_1^*$,

$$3(x_0 + 1 + y_0) - 2 - t_0 = -5 \pm \sqrt{\cos\alpha}\left(3\cos\left(\frac{\alpha}{2} - \beta\right) + \sin\left(\frac{\alpha}{2}\right) - \beta\right) - \sin\alpha < 0.$$

Therefore, F_2 and $(\partial_\infty I_1^+ \cup \partial_\infty I_1^\star)$ are separated by the above plane.

Table I gives the other curves we used.

Consider a curve C_+ in $\partial_\infty D_\Sigma - (\cup_{k\in\mathbb{Z}} A^k(E_B \cup E_{B^{-1}}))$ which consisting of eight edges:

(i) glue two copies of C_6 together along x_1;

(ii) take a copy C_{21}, C_{22}, C_{23}, and C_{24};

(iii) glue two copies of C_8 together along x_3.

These edges were then glued together along $AB^2(y_1)$, $A(w_3)$, $AB^2(y_2)$, and $A(w_4)$ to obtain the simple closed curve C_+ (the union of blue edges in Figure 9). Similarly, there is a curve $C_- = A^{-1}(C_+)$ that is the union of green edges in Figure 9.

https://doi.org/10.1017/S0305004126102163 Published online by Cambridge University Press

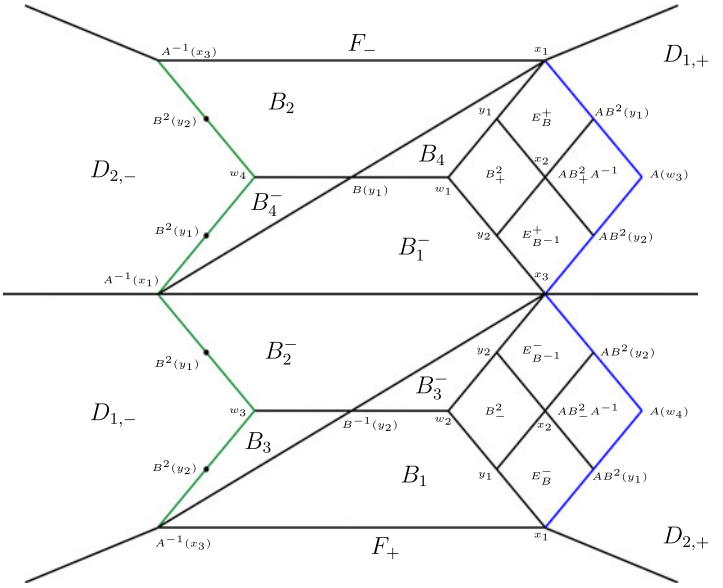


Figure 12. The boundary of the polytope N for $\Delta_{4,\infty,\infty;\infty}$.

PROPOSITION 4·9. *There are proper once punctured disks D_- and D_+ in the complement of the union of $\mathcal{S} \cup_{k\in\mathbb{Z}} A^k(E_B \cup E_{B^{-1}})$ in $\partial\mathbf{H}^2_{\mathbb{C}}$ such that*:

(i) *∂D_- is C_-;*
(ii) *∂D_+ is C_+;*
(iii) *$D_+ = A(D_-)$;*
(iv) *$D_- \cap F = C_{19}$;*
(v) *$D_+ \cap F = C_{20}$;*
(vi) *$D_+ \cap D_- = \emptyset$.*

Proof. With the boundary ∂D_- as stated in Proposition 4·9, then by Proposition 4·7, ∂D_- bounds a proper once punctured disk D_- in $\partial\mathbf{H}^2_{\mathbb{C}}$, the punctured point is q_∞. Let $D_+ = A(D_-)$. Since $\partial D_- \cap \partial D_+ = \emptyset$, by the standard argument in 3-manifold theory, we may assume $D_- \cap D_+ = \emptyset$. Moreover, we may isotope D_- such that $D_- \cap F = C_{19}$ and $D_+ \cap F = C_{20}$. We may also assume that the boundaries of D_- and D_+ are fixed during the isotopy.

5. 3-*manifold at infinity of* $\Delta_{4,\infty,\infty;\infty}$

In this section, we prove Theorem 1·2. In Section 4, it was proven that $\partial_\infty D_\Sigma - \cup_{k\in\mathbb{Z}} A^k(E_B \cup E_{B^{-1}})$ is a topologically A-invariant $(\mathbb{R}^2 - \mathbb{D}^2) \times \mathbb{R}$. Recall that $A(D_-) = D_+$, the once punctured disks D_- and D_+ separate $\partial_\infty D_\Sigma - \cup_{k\in\mathbb{Z}} A^k(E_B \cup E_{B^{-1}})$ into three parts, and exactly one of them, denoted as U, contains both D_- and D_+. Now U is homeomorphic to $(\mathbb{R}^2 - \mathbb{D}^2) \times [0, 1]$, which serves as a fundamental domain for the A-action. Moreover, the disk F from Subsection 4·2 cuts U into a 3-ball, denoted by N.

Figure 12 shows a 2-cell decomposition of the boundary 2-sphere of N. The curves C_- and C_+, which are unions of green and blue edges in Figure 8, now correspond to the green

https://doi.org/10.1017/S0305004126102163 Published online by Cambridge University Press

Table II. *2-cells and their edges*

Name	Edges	Name	Edges
B_1	$C_{17}, C_{15}, C_{28}, B^2A^{-1}(C_{22}), C_1$	B_1^{-1}	$C_{18}, C_7, B^2A^{-1}(C_{23}), C_{25}, C_{13}$
B_2	$C_{17}, C_{12}, A^{-1}(C_{24}), C_{26}, C_{14}$	B_2^{-1}	$C_{18}, C_{16}, C_{27}, A^{-1}(C_{21}), C_{11}$
B_3	$C_{15}, C_{12}, A^{-1}(C_{23}), C_{27}$	B_3^{-1}	$C_7, C_{16}, C_{28}, B^2A^{-1}(C_{24})$
B_4	$C_{25}, B^2A^{-1}(C_{21}), C_5, C_{14}$	B_4^{-1}	$A^{-1}(C_{22}), C_{26}, C_{13}, C_{11}$
B_+^2	$B^2A^{-1}(C_{21}), C_1, C_3, B^2A^{-1}(C_{23})$	$AB_+^2A^{-1}$	C_{21}, C_2, C_4, C_{23}
B_-^2	$B^2A^{-1}(C_{22}), C_1, C_3, B^2A^{-1}(C_{24})$	$AB_-^2A^{-1}$	C_{22}, C_2, C_4, C_{24}

and blue paths in Figure 12. In addition, by our choice of D_- and D_+, the region U contains only one half of $s_0^\star \cap \partial\mathbf{H}^2_{\mathbb{C}}$ and one half of $s_1^\star \cap \partial\mathbf{H}^2_{\mathbb{C}}$. The side-pairing between them is AB^2.

We list the relevant cells in Table II. The 2-cell decomposition of ∂N consists of the following parts:

(i) we divide $s_0^+ \cap \partial\mathbf{H}^2_{\mathbb{C}}$ into four subdisks B_1, B_2, B_3 and B_4, and divide $s_0^- \cap \partial\mathbf{H}^2_{\mathbb{C}}$ into four subdisks B_1^{-1}, B_2^{-1}, B_3^{-1} and B_4^{-1};

(ii) we divide $s_0^* \cap \partial\mathbf{H}^2_{\mathbb{C}}$ into disks B_+^2 and B_-^2, and divide $s_1^* \cap \partial\mathbf{H}^2_{\mathbb{C}}$ into two disks $AB_+^2A^{-1}$ and $AB_-^2A^{-1}$;

(iii) two copies of F, say F_+ and F_-;

(iv) two copies of E_B, say E_B^+ and E_B^-;

(v) two copies of $E_{B^{-1}}$, say $E_{B^{-1}}^+$ and $E_{B^{-1}}^-$;

(vi) we divide D_- into two disks $D_{-,1}$ and $D_{-,2}$, and divide D_+ into two disks $D_{+,1}$ and $D_{+,2}$.

By matching the edges of 2-cells in Table II, we have that $AB^2(B_-^2) = AB_-^2A^{-1}$, $AB^2(B_+^2) = AB_+^2A^{-1}$ and $B(B_i) = B_i^{-1}$ for $i = 1, 2, 3, 4$. We also have that $A(D_{-,1}) = D_{+,1}$ and $A(D_{-,2}) = D_{+,2}$.

Let M be the 3-manifold at infinity of the even subgroup Σ of $\Delta_{4,\infty,\infty;\infty}$, which is the quotient space of N. According to the above analysis, the side-pairings on N are

$$\begin{aligned}
f_1 = B : B_1 &\longrightarrow B_1^{-1},\\
f_2 = B : B_2 &\longrightarrow B_2^{-1},\\
f_3 = B : B_3 &\longrightarrow B_3^{-1},\\
f_4 = B : B_4 &\longrightarrow B_4^{-1},\\
f_5 = AB^2 : B_-^2 &\longrightarrow AB_-^2A^{-1},\\
f_6 = AB^2 : B_+^2 &\longrightarrow AB_+^2A^{-1},\\
f_7 = A : D_{1,-} &\longrightarrow D_{1,+},\\
f_8 = A : D_{2,-} &\longrightarrow D_{2,+},\\
f_9 : F_- &\longrightarrow F_+,\\
f_{10} : E_B^- &\longrightarrow E_B^+,\\
f_{11} : E_{B^{-1}}^- &\longrightarrow E_{B^{-1}}^+.
\end{aligned}$$

https://doi.org/10.1017/S0305004126102163 Published online by Cambridge University Press

Table III. *Edge cycles and relations for the 3-manifold at infinity of* $\Delta_{4,\infty,\infty;\infty}$

Edge	Edge cycle	Cycle relation
e_1	$e_1 \xrightarrow{f_9} e_{41} \xrightarrow{f_7} e_{21} \xrightarrow{f_8^{-1}} e_1$	$f_8^{-1}f_7f_9$
e_2	$e_2 \xrightarrow{f_2} e_{35} \xrightarrow{f_3^{-1}} e_{42} \xrightarrow{f_7} e_{19} \xrightarrow{f_{11}^{-1}} e_{22} \xrightarrow{f_8^{-1}} e_2$	$f_8^{-1}f_{11}^{-1}f_7f_3^{-1}f_2$
e_3	$e_3 \xrightarrow{f_2} e_{38} \xrightarrow{f_3} e_{33} \xrightarrow{f_5} e_{23} \xrightarrow{f_8^{-1}} e_3$	$f_8^{-1}f_5f_3f_2$
e_4	$e_4 \xrightarrow{f_2} e_{44} \xrightarrow{f_7} e_{12} \xrightarrow{f_6^{-1}} e_7 \xrightarrow{f_4} e_4$	$f_4f_6^{-1}f_7f_2$
e_5	$e_5 \xrightarrow{f_4} e_{48} \xrightarrow{f_8} e_{26} \xrightarrow{f_5^{-1}} e_{31} \xrightarrow{f_1} e_5$	$f_1f_5^{-1}f_8f_4$
e_6	$e_6 \xrightarrow{f_2} e_{45} \xrightarrow{f_7} e_{11} \xrightarrow{f_{10}^{-1}} e_{27} \xrightarrow{f_8^{-1}} e_{47} \xrightarrow{f_4^{-1}} e_6$	$f_4^{-1}f_8^{-1}f_{10}^{-1}f_7f_2$
e_8	$e_8 \xrightarrow{f_4} e_{49} \xrightarrow{f_1^{-1}} e_{29} \xrightarrow{f_{10}} e_8$	$f_{10}f_1^{-1}f_4$
e_9	$e_9 \xrightarrow{f_2} e_{36} \xrightarrow{f_1^{-1}} e_{40} \xrightarrow{f_9^{-1}} e_9$	$f_9^{-1}f_1^{-1}f_2$
e_{10}	$e_{10} \xrightarrow{f_9} e_{28} \xrightarrow{f_8^{-1}} e_{46} \xrightarrow{f_7} e_{10}$	$f_7f_8^{-1}f_9$
e_{13}	$e_{13} \xrightarrow{f_{10}^{-1}} e_{25} \xrightarrow{f_5^{-1}} e_{30} \xrightarrow{f_{10}} e_{14} \xrightarrow{f_6} e_{13}$	$f_6f_{10}f_5^{-1}f_{10}^{-1}$
e_{15}	$e_{15} \xrightarrow{f_6} e_{18} \xrightarrow{f_7^{-1}} e_{43} \xrightarrow{f_3} e_{37} \xrightarrow{f_1} e_{15}$	$f_1f_3f_7^{-1}f_6$
e_{16}	$e_{16} \xrightarrow{f_6} e_{17} \xrightarrow{f_{11}^{-1}} e_{24} \xrightarrow{f_5^{-1}} e_{32} \xrightarrow{f_{11}} e_{16}$	$f_{11}f_5^{-1}f_{11}^{-1}f_6$
e_{20}	$e_{20} \xrightarrow{f_{11}^{-1}} e_{34} \xrightarrow{f_3^{-1}} e_{39} \xrightarrow{f_1} e_{20}$	$f_1f_3^{-1}f_{11}^{-1}$

Using the side-pairings on ∂N, the edge cycles for the 3-manifold M are given in Table III. Then we get a presentation of the fundamental group of the 3-manifold M. It is a group $\pi_1(M)$ with eleven generators $f_1, f_2, \ldots, f_{11}$ and thirteen relations. Using Magma, we simplify this presentation to obtain:

$$\pi_1(M) = \left\langle x_1, x_2, x_3, x_4 \,\middle|\, \begin{matrix} x_4x_2^{-1}x_1x_4^{-1}x_1^{-1}x_2, \quad x_1x_4^{-1}x_3x_1^{-1}x_4x_3^{-1}, \\ x_4x_2x_1x_3x_2x_4^{-1}x_2^{-2}x_3^{-1}x_1^{-1} \end{matrix} \right\rangle,$$

where $x_1 = f_1$, $x_2 = f_2$, $x_3 = f_3$ and $x_4 = f_7$.

Let 8_1^4 be the 4-component chain link in SnapPy Census [2], it is hyperbolic with volume 10.1494160641 and

$$\pi_1\left(S^3 - 8_1^4\right) = \left\langle a, b, c, d \,\middle|\, ab^{-1}a^{-1}b, acb^{-1}da^{-1}c^{-1}bd^{-1}, acd^{-1}c^2a^{-1}c^{-1}dc^{-2} \right\rangle.$$

Using Magma, we find an isomorphism $\phi : \pi_1(M) \to \pi_1(S^3 - 8_1^4)$ given by $\phi : \pi_1(M) \to \pi_1(S^3 - 8_1^4)$ with

$$\phi(x_1) = c^{-1}b, \quad \phi(x_2) = c^{-1}, \quad \phi(x_3) = b^{-1}d, \quad \phi(x_4) = a.$$

The inverse isomorphism is $\phi^{-1} : \pi_1(S^3 - 8_1^4) \to \pi_1(M)$ with

$$\phi^{-1}(a) = x_4, \quad \phi^{-1}(b) = x_2^{-1}x_1, \quad \phi^{-1}(c) = x_2^{-1}, \quad \phi^{-1}(d) = x_2^{-1}x_1x_3.$$

By the prime decomposition theorem for 3-manifolds [11], M is the connected sum of $S^3 - 8_1^4$ and a closed 3-manifold L with trivial fundamental group. By the Poincaré

https://doi.org/10.1017/S0305004126102163 Published online by Cambridge University Press

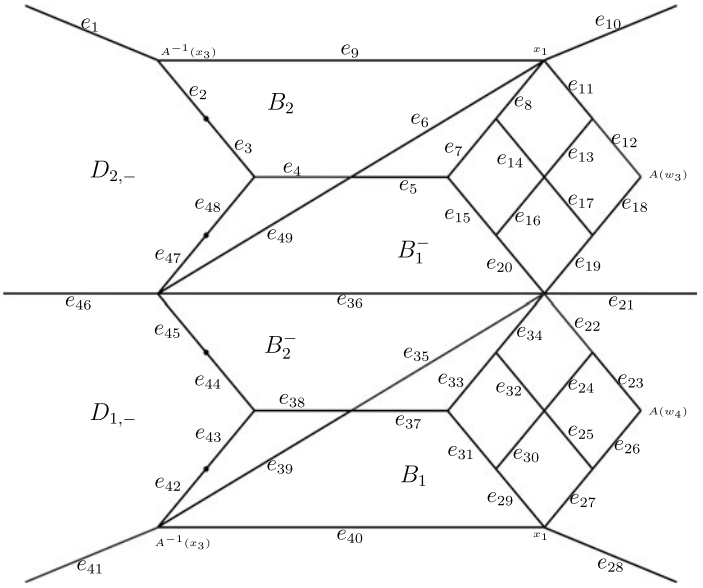


Figure 13. Edges in the 3-ball N for $\Delta_{4,\infty,\infty;\infty}$. Since there are too many vertices and 2-cells, we only provide a few of their labels in this figure. Their full labels are the same as Figure 12.

conjecture (now a theorem), it follows that L is the 3-sphere. Therefore, M is homeomorphic to $S^3 - 8_1^4$, which completes the proof of Theorem 1·2.

6. *A conjectural picture on $\Delta_{p,q,r;\infty}$ of type A*

This section discusses topics related to 3-manifolds associated with complex hyperbolic triangle groups that contain accidental parabolic elements. Our aim is to sketch a global conjectural picture of the 3-manifolds at infinity of the groups $\Delta_{p,q,r;\infty}$ for $3 \le p \le 9$.

6·1. *3-manifold at infinity of $\Delta_{p,\infty,\infty;\infty}$ for $3 \le p \le 9$*

In [14], Ma and Xie proved the following

THEOREM 6·1. *Let $\Gamma = \langle I_1, I_2, I_3 \rangle$ be the complex hyperbolic triangle group $\Delta_{3,\infty,\infty;\infty}$. Then the 3-manifold at infinity of the even subgroup $\langle I_1I_2, I_2I_3 \rangle$ of Γ is the magic 3-manifold in the SnapPy Census.*

The magic 3-manifold in the SnapPy Census [2] is the complement of the chain link 6_1^3 in the 3-sphere, which is hyperbolic with three cusps and volume 5.3334895669 numerically. Recall that we have proved that the 3-manifold at infinity of the even subgroup of $\Delta_{4,\infty,\infty;\infty}$ is the complement of the chain link 8_1^4 in the 3-sphere. Compared with the above results, we denote by M_p the 3-manifold at infinity of the even subgroup of $\Delta_{p,\infty,\infty;\infty}$ for $3 \le p \le 9$. Recall that Schwartz's conjecture in [26] predicts that this group is discrete, so M_p is well-defined. For $p \le 9$, the complex hyperbolic group $\Delta_{p,\infty,\infty}$ is of type A in the sense of Schwartz [26]. For more details, see [26]. We note that in the group $\Delta_{p,\infty,\infty;\infty} = \langle I_1, I_2, I_3 \rangle$ for $3 \le p \le 9$, I_1I_2, I_1I_3 and $I_1I_3I_2I_3$ are parabolic by definition. Moreover, one can verify that $I_1(I_3I_2)^kI_3$ is parabolic for any $2 \le k \le p-2$. Therefore, there are (at least) p conjugacy classes of parabolic elements in $\Delta_{p,\infty,\infty;\infty}$. In particular, there are (at least) $p-3$ hidden

https://doi.org/10.1017/S0305004126102163 Published online by Cambridge University Press

conjugacy classes of parabolic elements in $\Delta_{p,\infty,\infty;\infty}$ which are unexpected. We propose the following conjecture.

CONJECTURE 6·2. *For $3 \le p \le 9$, the 3-manifold M_p at infinity of the even subgroup of the complex hyperbolic triangle group $\Delta_{p,\infty,\infty;\infty}$ is the complement of the chain link C_p in the 3-sphere.*

Here for each $p \ge 3$, the chain link C_p is a hyperbolic link in S^3 with p components and crossing number $2p$. See page 144 of [29] for the diagrams of chain links. We note that chain links C_3, C_4 and C_5 are links 6_1^3, 8_1^4 and 10_1^5 respectively [2]. In Figure 1, we show the diagrams of C_4 and C_5. In other words, results in [14] and this paper are special cases of Conjecture 6·2. We also have strong evidence supporting Conjecture 6·2 for $p = 5$; a proof will appear in a subsequent paper.

6·2. 3-*manifold at infinity of* $\Delta_{p,q,r;\infty}$ *for* $3 \le p \le 9$

In [14], Ma and Xie proposed

CONJECTURE 6·3. *The 3-manifold at infinity of the even subgroup of the complex hyperbolic triangle group $\Delta_{3,m,\infty;\infty}$ is the hyperbolic 3-manifold obtained via the Dehn surgery of 6_1^3 on the first cusp with slope $m-2$. Moreover, the 3-manifold at infinity of the even subgroup of the complex triangle group $\Delta_{3,m,n;\infty}$ is the hyperbolic 3-manifold obtained by the Dehn fillings of 6_1^3 on the first two cusps with slopes $m-2$ and $n-2$ respectively.*

Note that in Conjecture 6·3 we use the meridian-longitude systems of the cusps of $S^3 - 6_1^3$ as in [16], which is different from the meridian-longitude systems in SnapPy. Results in [1, 3, 13, 14, 20] provided very strong evidence of Conjecture 6·3.

In [12], Jiang, Wang and Xie proved

THEOREM 6·4. *Let $\Gamma = \langle I_1, I_2, I_3 \rangle$ be the complex hyperbolic triangle group $\Delta_{4,4,\infty;\infty}$. Then the 3-manifold at infinity of the even subgroup $\langle I_1I_2, I_2I_3 \rangle$ of Γ is the 3-manifold s782 in the SnapPy Census.*

It is not difficult to show that $s782$ can be obtained by Dehn fillings on two cusps of $S^3 - 8_1^4$. So, the 3-manifold at infinity of $\Delta_{4,4,\infty;\infty}$ can be obtained from the 3-manifold at infinity of $\Delta_{4,\infty,\infty;\infty}$ by Dehn fillings on two cusps.

Motivated by the above, we propose

CONJECTURE 6·5. *For each $3 \le p \le 9$, there is a preferred thrice-cusped hyperbolic 3-manifold N_p, which is obtained by Dehn filling the $p-3$ cusps of M_p. Moreover, the 3-manifold at infinity of the even subgroup of the complex hyperbolic triangle group $\Delta_{p,q,r;\infty}$ is obtained by Dehn filling two cusps of N_p when $p < q < r$.*

Here, we assume $p < q < r$, so there is no obvious symmetry of the group $\Delta_{p,q,r;\infty}$. From the group $\Delta_{p,\infty,\infty;\infty}$ to the group $\Delta_{p,q,r;\infty}$, we first kill $p-3$ hidden conjugate classes of parabolic elements. This process corresponds to topological Dehn fillings from M_p to N_p. Then two more Dehn fillings on N_p should result in the 3-manifold at infinity of the even subgroup of $\Delta_{p,q,r;\infty}$. In particular, the manifolds M_3 and N_3 are the same. Thus, for $3 \le p \le 9$, the proposed 3-manifold $M_p = S^3 - C_p$ serves as a seed that generates numerous

https://doi.org/10.1017/S0305004126102163 Published online by Cambridge University Press

explicit 3-manifolds admitting spherical CR uniformisations. The authors have a preliminary conjecture regarding the 3-manifold N_p, but extensive computations are needed to substantiate it.

Acknowledgements. The authors would like to thank Nathan Dunfield for the helpful communication on SnapPy via email. We would also like to thank Fangting Zheng for the help with Magma. J. Ma was supported by the National Natural Science Foundation of China (No. 12171092). The second author is grateful to the LMNS (Laboratory of Mathematics for Nonlinear Science) of Fudan University for its financial support and hospitality during his visit. He was also supported by the National Natural Science Foundation of China (No. 12271148) and the Guangdong Basic and Applied Basic Research Foundation (No. 2025A1515011486), and acknowledges the Greater Bay Area Institute for Innovation, Hunan University, Guangzhou, China, where part of this work was completed.

REFERENCES

[1] M. ACOSTA. Spherical CR uniformisation of Dehn surgeries of the Whitehead link complement. *Geom. Topol.* **23** (2019), 2593–2664.
[2] M. CULLER, N. M. DUNFIELD, M. GOERNER and J. R. WEEKS. SnapPy, a computer program for studying the geometry and topology of 3-manifolds. http://snappy.computop.org.
[3] M. DERAUX and E. FALBEL. Complex hyperbolic geometry of the figure eight knot. *Geom. Topol.* **19** (2015), 237–293.
[4] M. DERAUX. On spherical CR uniformisation of 3-manifolds. *Exp. Math.* **24** (2015), 355–370.
[5] M. DERAUX. A 1-parameter family of spherical CR uniformisations of the figure eight knot complement. *Geom. Topol.* **20** (2016), 3517–3621.
[6] M. DERAUX, J. R. PARKER and J. PAUPERT. New non-arithmetic complex hyperbolic lattices. *Invent. Math.* **203** (2016), 681–771.
[7] E. FALBEL, G. FRANCSICS and J. R. PARKER. The geometry of the Gauss-Picard modular group. *Math. Ann.* **349**(2) (2011), 459–508.
[8] E. FALBEL, A. GUILLOUX and P. WILL. Slim curves, limit sets and spherical CR uniformisations. *Groups Geom. Dyn.* **18**(4) (2024), 1507–1557.
[9] W. M. GOLDMAN. *Complex Hyperbolic Geometry*. (Oxford University Press, Oxford, 1999).
[10] W. M. GOLDMAN and J. R. PARKER. Complex hyperbolic ideal triangle groups. *J. Reine Angew. Math.* **425** (1992), 71–86.
[11] J. HEMPEL. 3-*manifolds*. Reprint of the 1976 original (AMS Chelsea Publishing, Providence, RI, 2004).
[12] Y. JIANG, J. WANG and B. XIE. A uniformisable spherical CR structure on a two-cusped hyperbolic 3-manifold. *Algebr. Geom. Topol.* **23** (2023), 4143–4184.
[13] J. MA and B. XIE. Three-manifolds at infinity of complex hyperbolic orbifolds. *Preprint*: arXiv:2205.11167.
[14] J. MA and B. XIE. Spherical CR uniformisation of the magic 3-manifold. *Comm. Anal. Geom.* **32**(9) (2024), 2381–2465.
[15] J. MA and B. XIE. Figure-eight knot is always over there. *Preprint:* arXiv:2310.05408 [math.GT].
[16] B. MARTELLI and C. PETRONIO. Dehn filling of the "magic" 3-manifold. *Comm. Anal. Geom.* **14**(5) (2006), 969–1026.
[17] G. D. MOSTOW. On a remarkable class of polyhedra in complex hyperbolic space. *Pacific J. Math.* **86** (1980), 171–276.
[18] J. R. PARKER. Notes on complex hyperbolic geometry. University of Durham (2003). Available at https://maths.dur.ac.uk/users/j.r.parker/img/NCHG.pdf
[19] J. R. PARKER, J. WANG and B. XIE. Complex hyperbolic (3,3,*n*) triangle groups. *Pacific J. Math.* **280** (2016), 433–453.
[20] J. R. PARKER and P. WILL. A complex hyperbolic Riley slice. *Geom. Topol.* **21** (2017), 3391–3451.
[21] A. PRATOUSSEVITCH. Traces in complex hyperbolic triangle groups. *Geom. Dedicata* **111** (2005), 159–185.

https://doi.org/10.1017/S0305004126102163 Published online by Cambridge University Press

[22] D. ROLFSEN. Knots and links. *Mathematics Lectures Series* **7** (Publish or Perish, Berkeley, CA, 1976).
[23] R. E. SCHWARTZ. Ideal triangle groups, dented tori, and numerical analysis. *Ann. of Math. (2)* **153**(3) (2001), 533–598.
[24] R. E. SCHWARTZ. A better proof of the Goldman-Parker conjectures. *Geom. Topol.* **9** (2005), 1539–1601.
[25] R. E. SCHWARTZ. Degenerating the complex hyperbolic ideal triangle groups. *Acta Math.* **186**(1) (2001), 105–154.
[26] R. E. SCHWARTZ. Complex hyperbolic triangle groups. Proceedings of the International Congress of Mathematicians, vol. 1. Invited Lectures (2002), 339–350.
[27] R. E. SCHWARTZ. Spherical CR geometry and Dehn surgery. *Annals of Mathematics Studies*, 165 (Princeton University Press, Princeton, NJ, 2007).
[28] J. M. THOMPSON. Complex hyperbolic triangle groups. PhDS. thesis. Durham University (2010).
[29] W. P. THURSTON. The geometry and topology of three-manifolds. http://www.msri.org/publications/books/gt3m

https://doi.org/10.1017/S0305004126102163 Published online by Cambridge University Press